Available online at www.sciencedirect.com

ScienceDirect

Geochimica et Cosmochimica Acta 197 (2017) 396–416

Geochimica et Cosmochimica Acta

www.elsevier.com/locate/gca

# Formation of non-magmatic iron-meteorite group IIE

John T. Wasson

*Department of Earth, Planetary and Space Sciences and Department of Chemistry and Biochemistry, University of California, Los Angeles, CA 90095-1567, USA*

Received 14 November 2015; accepted in revised form 25 September 2016; available online 29 October 2016

**Abstract**

Instrumental neutron-activation (INAA) data for metal in 22 nonmagmatic IIE meteorites show narrow ranges in Ir and other refractory siderophiles; the Ir range is a factor of 2.6, a factor of ~2 smaller than in nonmagmatic IAB-MG, and orders of magnitude smaller than in the large magmatic groups. Siderophile data show no evidence of fractional crystallization. IIE irons can be split into two sets, a larger main-set and a set of 6 Cu- (or FeS) rich irons. Elemental concentrations in metal from veins in H5 chondrite Portales Valley fall within the IIE range with the exceptions of Co (high) and Ga (low).

H-group-chondrite and Au-normalized IIE abundances for siderophiles show that IIE irons are ~30% higher than H in refractory siderophiles Re, Ir and W and are about 30% lower than H chondrites in the volatiles Ga and Sb, inconsistent with proposals that IIE irons formed from H chondrites. The IIE fractionations contrast with those in L chondrites which are about 15% lower than H in the three refractory elements and 40% higher than H in volatiles indicating that IIE irons did not form from H chondrites but from a more reduced and siderophile-rich kind of ordinary chondrite ("HH" chondrites). Most O-isotope data support a close relationship between IIE irons and H or HH chondrites; lower $\Delta^{17}O$ in primitive (chondritic) silicates support an HH classification. Literature isotopic data for Ru and Mo also show that IIE metal formed from an ordinary chondrite parent; it appears that the silicates and metal were formed by melting of a single asteroid. There is no evidence for radiogenic ($^{26}Al$) heating; this, the rapid cooling recorded in the sizes of parental gamma crystal in the metal and the absence of fractional crystallization strongly support the hypothesis that IIE melting was the result of impacts.

To summarize, the weight of the evidence favors the conclusion that IIE meteorites were formed by one or more impacts on an HH asteroid. The target probably had a composition like the chondritic materials in Netschaevo, but was unequilibrated and had much higher porosity.


*Keywords:* Elemental composition; HH-chondrites; Source of IIE irons; Non-magmatic iron; Meteorites; Impact heating

## 1. INTRODUCTION

There are two sets of nonmagmatic irons characterized by the presence of chondritic or chondrite-related silicates and the absence of fractional crystallization trends in their metal: the IAB complex (Wasson and Kallemeyn, 2002), consisting of the large main group of IAB (IAB-MG) and several closely related subgroups, and the small group IIE (Wasson, 1970; Scott and Wasson, 1976; Wasson and Wang, 1986). This paper provides a significant augmentation of compositional data for IIE metal and reviews isotopic and petrographic properties of the group Table 1.

Although all recent papers infer that impacts played a major role in IIE formation, some (e.g., Ruzicka et al., 1999; Ruzicka, 2014) note evidence for an earlier melting episode that they attribute to $^{26}Al$ heating. Others (e.g., Wasson and Wang, 1986) stress that radiogenic heating tends to produce central cores and attribute all heating to impacts.

*E-mail address:* jtwasson@ucla.edu

http://dx.doi.org/10.1016/j.gca.2016.09.043
0016-7037/

A major difference between the IAB-MG and IIE groups is that a large fraction of IIE silicates are globular; they appear to have formed as rapidly cooled (largely) albitic melts whereas the IAB-MG silicates are commonly angular and roughly chondritic in composition, with many showing only minor loss or gain of low-melting S-rich-metal and alkali-rich-silicate-melt fractions.

It was the similarity in the mineral assemblages that led Bunch et al. (1970) to group Weekeroo Station, Colomera and Kodaikanal together as Weekeroo-Station type inclusions. Stimulated by this study of the silicate inclusions Wasson (1970) studied Ni, Ga, Ge and Ir in the metal of these three irons and showed them to have similar compositions. He also showed that metal in Elga, which has similar plagioclase-rich inclusions, has a similar composition. Similar metal compositions were also observed in metal from Netschaevo, which has chondritic inclusions, and in Barranca Blanca and Arlington, which do not contain silicate inclusions.

Globular IIE silicates commonly consist of plagioclase-rich silicates and glass that are generally inferred to have formed by low-degree melting of chondritic matter. In one anomalous IIE, Netschaevo, the silicates are chondritic (Bild and Wasson, 1977); the inclusions in Techado (Casanova et al., 1995) and Watson (Olsen et al., 1994) have high contents of mafic minerals and are roughly chondritic in composition. Rare chondrules have been found in Netschaevo silicates (Olsen and Jarosewich, 1971), in Mont Dieu (Van Roosbroek et al., 2015) and in Garhi Yasin (McDermott et al., 2015); the latter observations imply that some Mont Dieu and Garhi Yasin silicates also have retained chondritic bulk compositions. A complication is that Van Roosbroek et al. (2016) recently discovered an impact-melt clast in Netschaevo.

Olsen and Jarosewich (1971) reported that Netschaevo olivine is Fa14, below the H-chondrite range; their bulk-chemical analysis showed the chondritic blocks to have a composition similar to that of H chondrites, but more reduced and richer in Fe and Ni. Neutron-activation elemental data by Bild and Wasson (1977) showed that Netschaevo silicate blocks are compositionally similar to H chondrites but are richer in siderophiles. They thus classified the chondritic silicates as HH, the most reduced and siderophile-rich members of the ordinary chondrite continuous-fractionation sequence. Clayton and Mayeda (1996) reported a $\Delta^{17}O$ value of 0.57‰ in Netschaevo, similar to the lowest values observed in the H group, consistent with this HH designation. More recent $\Delta^{17}O$ data for Netschaevo show it to be resolvably below the H-chondrite field (McDermott et al., 2015).

These closely related irons were christened group IIE by Scott and Wasson (1975, 1976). These papers also included some irons that are now recognized to be too deviant to include in the group. Malvin et al. (1984) showed that Seymchan (now known to be a main-group pallasite) and Lonaconing are not members of group IIE. Wasson and Wang (1986) confirmed this, and concluded that Leshan should be included in the group as its most Ni-rich member (our data are based on sawings; the main mass of Leshan is currently misplaced).

This is our first IIE paper to follow the now preferred practice of plotting metal elemental concentration data against Au rather than Ni (both elements are incompatible but Au is more precisely determined and shows a larger compositional range than Ni); our data are more accurate and precise than those of Wasson and Wang (1986) and we add data for 10 additional IIE meteorites. We have not studied three other IIE irons, Sahara 03505 (D'Orazio et al., 2009), the tiny RBT 04186 (4.5 g; classification based on silicate mineralogy, Meteoritical Bull. 92) and NWA 6716 (data obtained by D'Orazio in Meteoritical Bull. 100). This brings the IIE total to 24. The observed fall Kavarpura (Meteoritical Bull. 100) was initially classified IIE but a more recent study reclassified it IVA (Ray et al., 2014).

A number of the recent additions to group IIE are small (<100 g) irons recovered from deserts (NWA 5608, SAH 03505 (SAH), MET 00428 (MET), TYR 05181 (TYR)) but some with similar textures are large (e.g., the largest mass of Mont Dieu weighs 430 kg, the only mass of Miles weighs 265 kg).

## 2. NEUTRON-ACTIVATION TECHNIQUES AND SAMPLES

We currently determine 16 elements (15 plus Fe) in metal by instrumental neutron-activation analysis (INAA) in replicate analyses; data for Fe are used for internal normalization. If sufficient material was available we analyzed all meteorites in duplicate in separate irradiations. Several years ago we started to determine Ru and Os but only a few IIE data are available. Only a minor fraction of the Ge and Sb data reported here were obtained by INAA; most were determined by radiochemical neutron-activation analysis (RNAA). With INAA our 95% error limits for Ge means are about ±12% at IIE levels near 65 μg/g; INAA Sb means have similar precisions at concentration levels near 150 ng/g.

We analyze meteorites two or more times to improve the precision and to control for gross sampling errors. The procedures are those given by Wasson et al. (1989) except for two minor changes. The mean sample thickness is now 3.0 instead of 3.2 mm, and we now apply small (generally in the range 0.95–1.05) sample-specific geometric corrections to make data from the first and second counts agree better with those from the third and fourth counts (which are corrected to make Fe + Ni = 990 mg/g). We minimize contamination of our samples by careful preparation and by a brief etching with a dilute mix of HCl and $HNO_3$ following the irradiation.

Although the INAA data were gathered over almost four decades, significant improvements in the quality were achieved starting in 1986. As a result, some meteorites were restudied and the recent analyses given extra (1.5× to 2×) weight in the determination of the means. In some meteorites we had previously determined Ni by atomic-absorption spectrophotometry; in these cases the Ni means are calculated treating the previous mean as an additional replicate. We have now recalculated older INAA runs to incorporate these more sophisticated correction procedures.

We did not use Filomena as a standard in our oldest runs; instead we irradiated aliquots of standardized solutions, a technique that was less reproducible. In our recalculations we have used newer analyses of some of the irons in these earlier runs to restandardize the data; in most cases concentrations changed by less than 5% relative.

Relative 95% confidence limits on the means are estimated to be means to be 1.5–3% for Co, Ni, Ga, Ir and Au, 4–6% for As and (RNAA) Ge, 7–10% for Ru (values >2 μg/g), W (values > 0.3 μg/g), Sb (>200 ng/g), Re (>50 ng/g) and Pt (>2 μg/g). Because much of the Cr is in minor phases (mainly chromite), sampling errors result in relative confidence limits on the mean ⩾ 10%. In addition, there is an Fe interference in the determination of Cr resulting from the $^{54}Fe(n,\alpha)^{51}Cr$ fast-neutron reaction that adds the equivalent of ~5 μg Cr per g of Fe. Our data were not corrected for this interference.

In runs carried out during the past 2 decades we used three INAA standards, two of which are IIAB irons, the Filomena specimen of the North Chile shower and a Coahuila specimen off an undetermined mass of this shower. We find Filomena to be a very uniform iron, and thus well suited to be a standard. Only Cr shows moderate scatter (a standard deviation of about 10% relative). Coahuila is slightly more variable in its composition, but is adequately uniform for use as a secondary standard. Our third standard is the NBS steel 809B which is quite uniform in composition; NBS 809B is our main standard for Sb and Cr and a secondary standard for As and W. The high Mn content of NBS 809B makes it too radioactive to include in the first count several hours after the end of an irradiation. Concentration data for these standards are given in electronic annex EA-4 of Wasson et al. (2007).

## 3. COMPOSITION AND PETROGRAPHY

### 3.1. Metal and metal–silicate textures in IIE

Metallographic structures reflect both high-temperature and low-temperature histories. The dimensions of the

Table 1
Assignments of IIE irons into compositional sets and compilation of sources, structures and inclusions. Kamacite width (k.w.) in units of mm.

| Meteorite | | Source | Cat. No. | k.w. | silic | troil | schrb | phos | References |
|---|---|---|---|---|---|---|---|---|---|
| *Main set* | | | | | | | | | |
| Arlington | Arl | SI | 627 | 0.8 | 0 | 0 | 0 | | Buchwald75 |
| Colomera | Col | MNCN | | 0.7 | 3 | 1 | 2 | | Buchwald75 |
| EET 83390 | EET | MWG | 2 | 1 | 0 | 0 | 1 | | Meteoritical Bull. |
| Elga | Elga | VIM | | 0.05 | 2 | 1 | 1 | 0 | Osadchii81 |
| Garhi Yasin | GarY | NHML | 1924,832 | 1 | 1 | 0 | 1 | | Buchwald75 |
| Kodaikanal | Kod | FMNH | Me574A4 | 0.1 | 3 | 1 | 2 | | Bence69;Buchwald75 |
| Leshan | Les | IGC | | | | | | | No information |
| Miles | Mil | SML | | 2 | 3 | 1 | 1 | | Ikeda97; Ruzicka10 |
| Netschaevo | Ntsch | FMNH | Me1154 | 1.2 | 3 | 1 | 1 | | Buchwald75 |
| Tarahumara | Tar | UCLA | | 0.1 | 2 | | | | This work |
| Techado | Tec | UNM | | 0.6 | 2 | 1 | | | Casanova95 |
| Tobychan | Tob | VIM | 15071 | 2.4 | 0 | 1 | 2 | | Ivanova76 |
| Verkhne Dnieprovsk | VeDn | NHML | 51183 | 0.07 | 0 | 1 | 2 | | BuchwaldClar87 |
| Watson | Wat | UCLA | 1302 | 0.07 | 3 | 0 | 1 | | This work |
| Weekeroo Station | WkSt | CalTech | | 2.5 | 3 | 1 | 1 | | Buchwald75 |
| *Cu-rich set* | | | | | | | | | |
| Barranca Blanca | BrBl | NHML | 41187 | 2 | 0 | 3 | 1 | 1 | Buchwald75 |
| HOW 88403 | HOW | MWG | 10, 6 | <0.1 | 0 | 3 | 2 | | Meteoritical Bull. |
| MET 00428 | MET | MWG | 4 | 0.1 | 0 | 3 | 0 | | Meteoritical Bull. |
| Mont Dieu | MtDi | MNHNP | | 0.5 | 2 | 3 | 1 | | VRoosbroek15; this work |
| Prospector Pool | ProP | WAM | | | 0 | 3 | | | This work |
| TYR 05181 | TYR | MWG | 7 | 0.8 | 3 | 3 | | | Meteoritical Bull. |
| *Other IIE* | | | | | | | | | |
| NWA 6716 | 6716 | | | | | 3 | 2 | 2 | Meteoritical Bull. |
| SAH 03505 | SAH | | | <0.1 | 0 | 3 | | 1 | D'Orazio09 |
| *Ambiguous* | | | | | | | | | |
| NWA 5608 | 5608 | | | | | | | | No information |

*Source abbreviations:* CalTech: California Inst. Technology, Pasadena; FMNH: Field Mus. Natural History, Chicago; IGC, Institute of Geochemistry, Acad. Sinica, Guiyang; MNCN: Mus. Nacional Ciencias Naturales, Madrid; MNHNP: Mus. National d'Histoire Naturelle, Paris; MWG: Meteorite Working Group; NHML, Nat. History Museum, London; SI, U. S. National Mus., Smithsonian Inst., Washington; SML, Southwest Meteorite Lab, Payson, AZ; UNM, Univ. New Mexico; UWS, Univ. Washington Seattle; VIM, Vernadsky Institute, Moscow; WAM, Western Australia Mus., Perth.
*Inclusion abundance:* 3, ⩾4%; 2, 0.5–3%; 1, 0.08–0.5%; 0, <0.08% (and not observed).
*Reference abbreviations:* Bence69, Bence and Burnett (1969); Buchwald75, Buchwald (1975); BuchwaldClar87, Buchwald and Clarke (1987); Casanova95, Casanova et al. (1995); D'Orazio09, D'Orazio et al. (2009); Ikeda97, Ikeda et al. (1997); Ivanova76, Ivanova and Kuznetsova (1976); Osadchii81, Osadchii et al. (1981); Ruzicka10, Ruzicka and Hutson (2010); VRoosbroek15, Van Roosbroek et al. (2015).

region with a continuous Widmanstätten pattern show the size of the parental $\gamma$ regions that formed as the metal cooled from the liquidus temperature around 1650–1700 K down to the temperature of $\alpha$ nucleation at about 1100 K. Because diffusion rates increase exponentially with temperature, most crystal growth occurs at high temperatures in a body cooling at a monotonic rate. However, impact-produced magmas commonly cooled much more rapidly at high temperatures and much of the growth may have occurred at intermediate temperatures.

As summarized in Table 2, the IIE irons show a wide spectrum of metallographic structures and a wide variety in the nature and abundance of inclusions. Some such as Weekeroo Station contain abundant silicates and have very little troilite and schreibersite. Others such as Prospector Pool and MET 00428 have abundant troilite but no recognized silicates or schreibersite. Buchwald (1975) observed neither silicates nor opaque inclusions (excepting one tiny chromite) in Arlington. It was because of this that Wasson and Wang (1986) designated it to be an anomalous IIE. Because it fits all the compositional trends of the group, I now find it best to treat it as a normal member of a relatively heterogeneous group.

Several IIEs have structures that record impact heating and shear followed by rapid cooling that produced fine metallic structures. Elga, Kodaikanal, Watson, Mont Dieu and Tarahumara have kamacite lamellae <0.2 mm thick similar to finest octahedrites (Off). Because the Ni contents are low, these very fine structures indicate rapid cooling. Interestingly, two meteorites with very fine kamacite (Kodaikanal and Watson) have low formation ages; Netschaevo, with coarse kamacite, also has a young

Table 2
Mean concentrations of 13 elements in IIE meteorites; meteorites arranged into sets. The first set (the main set) consists of irons we are treating as normal although some elements show concentrations >3 s outside the mean. The second set consists of seven high Cu irons that have data for several elements outside the main-set range on element-Au diagrams. The next set is a IIE iron for which data are of lower quality (NWA 5608) and the next consists of data for two analyses of H5 Portales Valley metal veins. The final two meteorites were not studied at UCLA and thus potentially systematically lower or higher for some elements (SAH 0305). This table available in digital form in the electronic annex.

| Meteorite | Cr µg/g | Co mg/g | Ni mg/g | Cu µg/g | Ga µg/g | Ge µg/g | As µg/g | Sb ng/g | W µg/g | Re ng/g | Ir µg/g | Pt µg/g | Au µg/g | srce | No. |
|---|---|---|---|---|---|---|---|---|---|---|---|---|---|---|---|
| *Main set* | | | | | | | | | | | | | | | |
| Arlington | <15 | 4.48 | 83.5 | 281 | 21.5 | 64.9 | 14.8 | | 1.20 | 820 | 7.41 | | 1.441 | IN | 0932 |
| Colomera | 16 | 4.51 | 75.5 | 172 | 27.3 | 71.2 | 7.99 | | 1.43 | 820 | 7.95 | | 0.940 | IN | 0372 |
| EET 83390 | 20 | 4.45 | 83.1 | 228 | 27.8 | 68.2 | 11.7 | 191 | 1.15 | 421 | 3.86 | 9.6 | 1.170 | IN | 1193 |
| Elga | 89 | 4.60 | 80.7 | 192 | 23.8 | 71.0 | 10.6 | <100 | 1.12 | 460 | 4.24 | 9.8 | 1.157 | UCLA | 1389 |
| Garhi Yasin | 11 | 4.39 | 80.3 | 218 | 22.0 | 65.3 | 10.2 | | 1.19 | 480 | 5.22 | | 1.123 | IN | 1080 |
| Kodaikanal | 128 | 4.59 | 80.5 | 184 | 21.1 | 68.7 | 11.5 | | 1.17 | 490 | 5.63 | | 1.245 | IN | 0239 |
| Leshan | 14 | 4.51 | 96.7 | 326 | 20.0 | 68.9 | 17.7 | 490 | 1.19 | 484 | 4.29 | | 1.785 | IN | 1155 |
| Miles | 10 | 4.43 | 79.6 | 182 | 26.7 | 71.1 | 9.52 | 110 | 0.86 | 100 | 1.12 | 4.1 | 1.129 | UCLA | 1363 |
| Netschaevo | 31 | 4.46 | 87.0 | 263 | 25.4 | 64.9 | 12.7 | 210 | 1.23 | 423 | 3.24 | 8.7 | 1.336 | IN | 0829 |
| Tarahumara | 72 | 4.66 | 80.0 | 168 | 27.1 | 78.7 | 10.3 | 130 | 1.33 | 574 | 4.89 | 11.7 | 1.124 | IN | 1551 |
| Techado | 20 | 4.47 | 90.5 | 309 | 23.4 | 70.2 | 16.3 | 378 | 1.01 | 596 | 5.37 | | 1.609 | IN | 1020 |
| Tobychan | 12 | 4.36 | 75.6 | 174 | 27.4 | 74.9 | 7.40 | | 1.22 | 650 | 6.53 | | 0.886 | IN | 0738 |
| TYR 05181 | 13 | 4.39 | 78.9 | 292 | 23.4 | | 9.54 | 185 | 1.22 | 669 | 6.56 | 10.5 | 0.983 | IN | 1981 |
| [a]Verkhne Dnieprov. | 28 | 4.74 | 86.4 | 187 | 23.4 | 70.3 | 11.7 | | 1.27 | 645 | 6.90 | | 1.330 | IN | 1122 |
| Watson | 58 | 4.58 | 80.7 | 157 | 25.6 | 66.3 | 11.9 | 153 | 1.12 | 670 | 6.32 | 9.9 | 1.271 | UCLA | 1302 |
| Weekeroo Station | 11 | 4.24 | 72.6 | 218 | 26.3 | 67.0 | 5.86 | | 0.96 | 306 | 3.06 | | 0.831 | IN | 0116 |
| *Cu-rich set* | | | | | | | | | | | | | | | |
| Barranca Blanca | 260 | 4.27 | 80.9 | 341 | 22.7 | 63.8 | 10.6 | 250 | 1.08 | 518 | 5.72 | | 1.136 | IN | 0138 |
| HOW 88403 | 812 | 4.34 | 86.1 | 382 | 22.1 | 53.2 | 11.9 | 360 | 0.96 | 545 | 4.70 | 8.0 | 1.250 | IN | 1372 |
| MET 00428 | 62 | 4.45 | 89.4 | 345 | 14.9 | 67 | 11.9 | 238 | 0.96 | 403 | 3.85 | 8.7 | 1.215 | In | 1815 |
| Mont Dieu | 300 | 4.38 | 79.3 | 329 | 24.8 | 60.5 | 8.60 | 220 | 1.02 | 570 | 4.97 | 9.1 | 0.884 | IN | 1548 |
| Prospector Pool | 330 | 4.35 | 89.4 | 397 | 22.7 | <150 | 12.2 | 180 | 0.97 | 520 | 4.45 | 9.2 | 1.227 | IN | 1926 |
| [a]RBT 04162 | 1197 | 4.05 | 85.1 | 457 | 21.8 | 419 | 11.3 | 209 | 0.83 | 463 | 3.90 | 7.6 | 1.130 | IN | 1935 |
| TYR 05181 | 13 | 4.39 | 78.9 | 292 | 23.4 | | 9.54 | 185 | 1.22 | 669 | 6.56 | 10.5 | 0.983 | IN | 1981 |
| *Ambiguous* | | | | | | | | | | | | | | | |
| [a]NWA 5608 | 315 | 4.75 | 85.4 | 248 | 28.3 | | 13.1 | 114 | 1.04 | 415 | 3.77 | 9.0 | 1.322 | IN | 2042 |
| *Chondr. metal vein* | | | | | | | | | | | | | | | |
| Portales Valley | 436 | 5.27 | 88.9 | 309 | 16.7 | | 13.9 | 297 | 0.9 | 365 | 3.27 | 7.7 | 1.349 | UCLA | 1456 |
| Portales Valley | 56 | 4.93 | 105 | 428 | 19.1 | | 13.8 | 409 | 1.1 | 403 | 3.49 | 7.4 | 1.506 | UCLA | 1456 |
| *Literature* | | | | | | | | | | | | | | | |
| Sahara 03505 | | 4.39 | 85.1 | 341 | 21.2 | 32.5 | 11.2 | 310 | 0.63 | 380 | 3.55 | 0.78 | 1.000 | | |

*Ru and Os values (in µg/g):* Prospector Pool, 7.4 Ru; NWA 5608 8.2 Ru 4.2 Os; TYR 05181, 10.1 Ru.
[a] Only one analysis of NWA 5608, RBT 04186 and Verkhne Dnieprovsk.

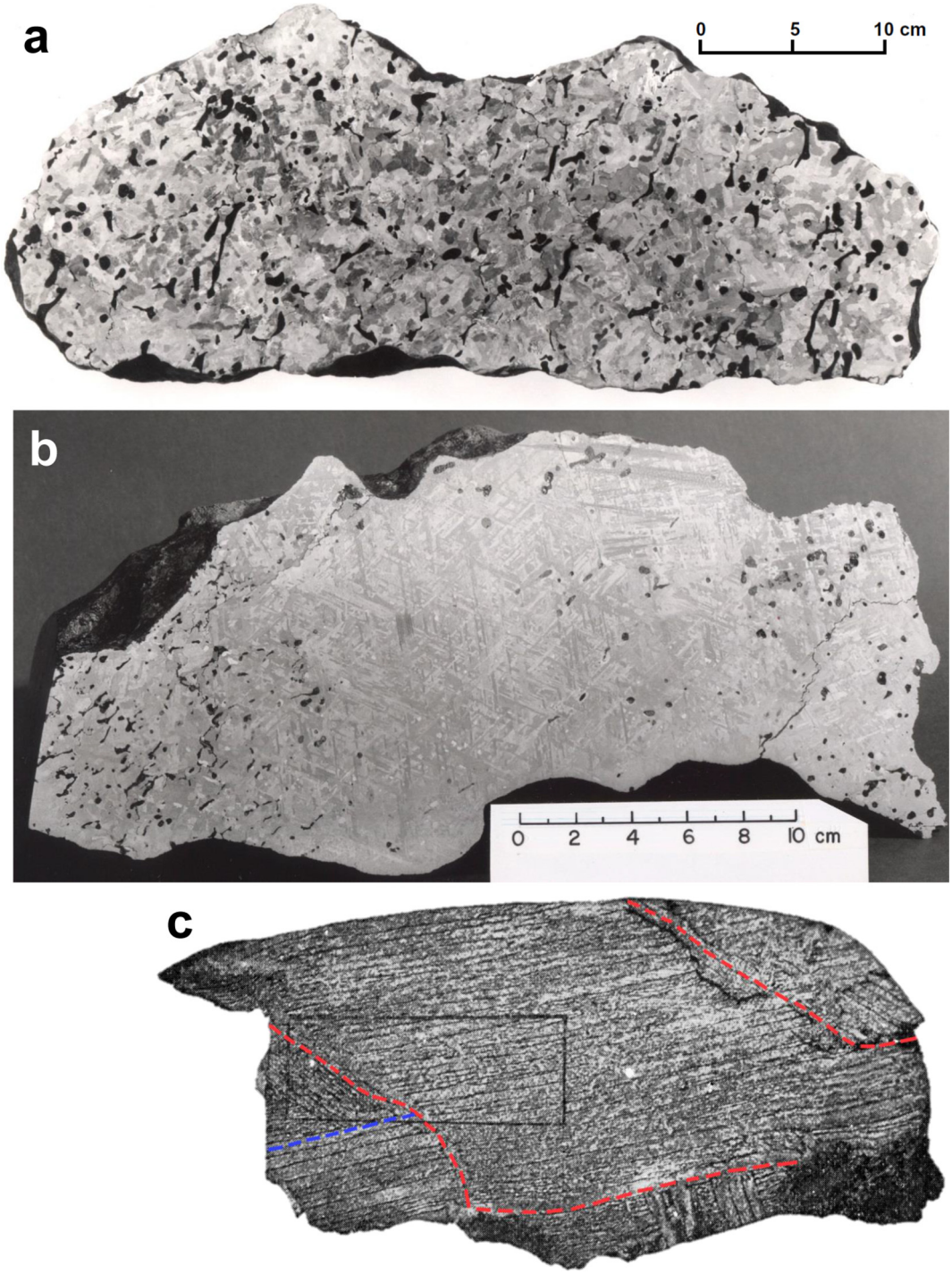


Fig. 1. Images of IIE structures. (a) Section of Weekeroo Station; silicate inclusion shapes range from spheroids to stringers oriented roughly up–down (Smithsonian image). (b) Section of Colomera; a central region is relatively silicate free, the left region shows silicate stringers oriented roughly SW–NE, and in the right region silicates form ellipsoids (Caltech image). (c) Several small parental gamma regions are delimited in this annotated mage of Arlington copied from the Winchell (1896) paper. Note that kamacite bands all tend to be parallel. Long dimension about 6 cm.

formation age (Olsen et al., 1994); there are no age data for Mont Dieu.

Buchwald (1975) makes the point that the $\gamma$ crystals (that formed by gradual growth at high temperatures and are parental to the octahedral structure) in IIE irons are commonly small. Typical sizes are 2–4 cm, as observed in Weekeroo Station by Buchwald (1975); Fig. 1a shows the Smithsonian slab examined by Buchwald. The largest

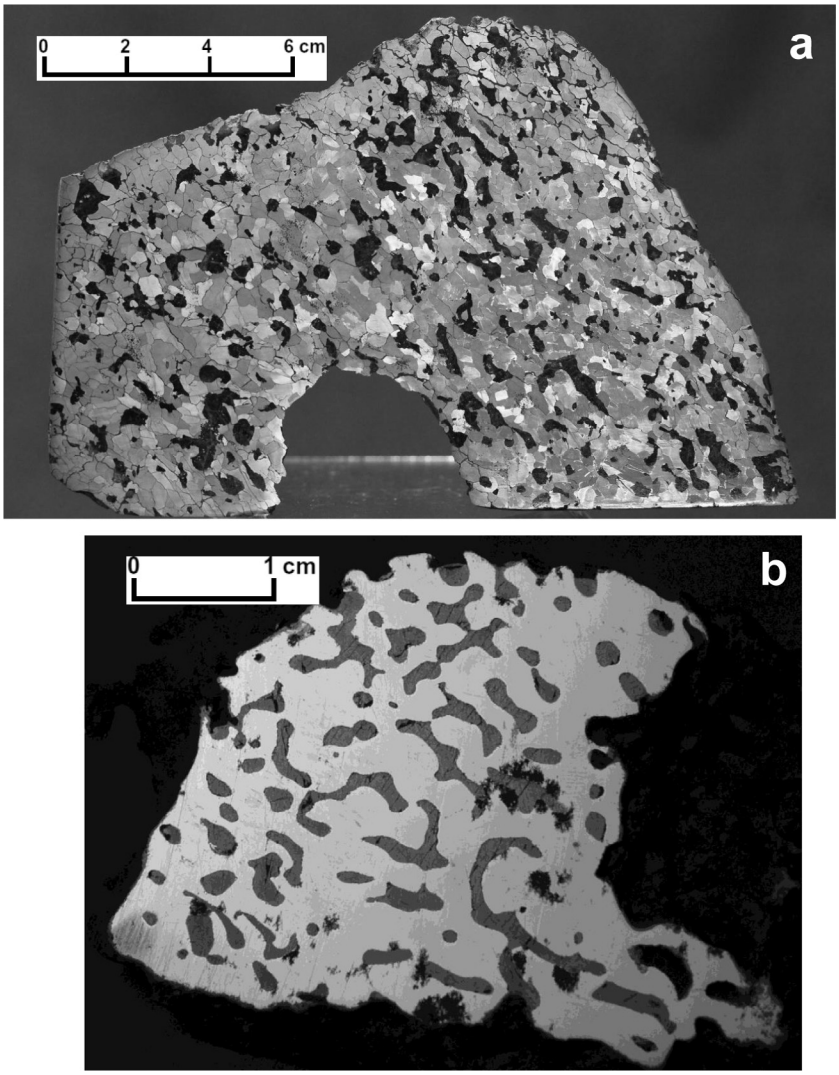


Fig. 2. Images of IIE structures. (a) Large section of Miles showing a high abundance of large, irregular globules; although the kamacite is relatively coarse (bandwidths about 2 mm), there are no patches > 2 cm showing octahedral orientations. M. Killgore image. (b) Small section of Prospector Pool; the troilite content is high (~20 vol% according to MB94) but silicate and schreibersite inclusions are absent or nearly so. Western Australian Museum image.

$\gamma$ region I have recognized in IIE irons is a 10 cm patch in the upper center of Colomera (Fig. 1b). Fig. 1c shows an image of Arlington from Winchell (1896); positions of the parental $\gamma$ boundaries inferred on the basis of changes in octahedral orientations are marked. Their sizes are 2–3 cm.

The largest precursor $\gamma$ region recognizable in the Miles section (Fig. 2a) is ~2 cm and M. Killgore, the owner of several large slabs, tells me dimensions of the parental $\gamma$ in these other sections are similar in size. Thus, with one exception, precursor $\gamma$ sizes are far smaller than those in magmatic irons (those in IVA irons are about 40 cm, those in the IIIAB Cape York are about 2 m).

No modern metallographic cooling rate estimates have been published for group IIE. A number of IIE irons (e.g., Weekeroo Station) have relatively coarse kamacite consistent with cooling rates through the $\alpha + \gamma$ field (800–1000 K) at rates inferred to be similar to those in most IIIAB irons (estimated to have cooled at rates of 10 K/Ma, Yang and Goldstein, 2006). Others with similar Ni contents mentioned above have much narrower kamacite lamellae implying cooling rates orders of magnitude higher.

Ruzicka et al. (1999) give arguments for rapid cooling of Weekeroo Station silicates at high temperatures. Some inclusions contain glass compositions that required cooling to 1270 K within 20 h and to 1120 K within 80 h. The high closure temperatures (1270–1370 K) observed in pyroxenes also require relatively rapid cooling, and thus much higher than those that produced the coarse Widmanstätten pattern at temperatures around 800 K.

### 3.2. Silicate, metal and troilite textural and petrographic observations

The classic textures of IIE silicates are nicely illustrated in the large sections of Weekeroo Station (Fig. 1a), Colomera (Fig. 1b) and Miles (Fig. 2a); they are globular and

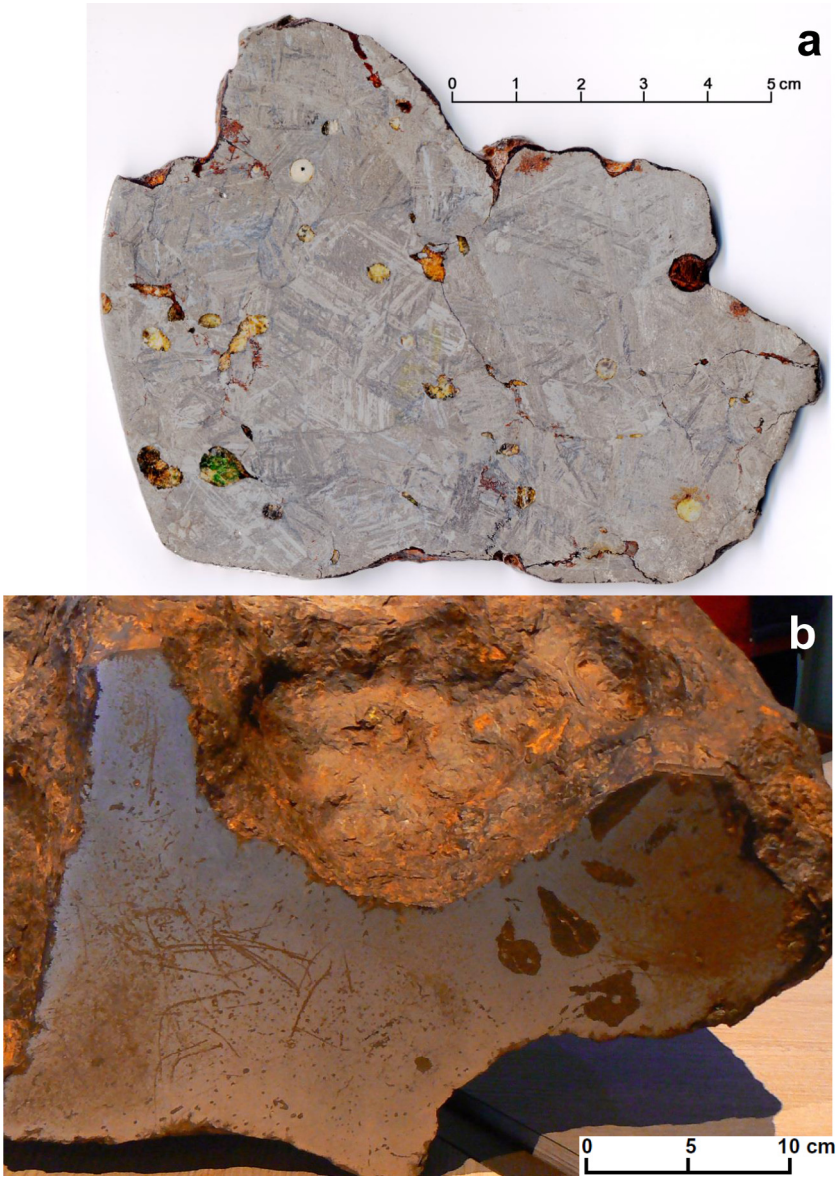


Fig. 3. Color images of IIE structures. (a) Small section of Tarahumara; in contrast to "typical" IIE silicates, the inclusions are a mix of igneous and crystalline (perhaps not melted during the impact event that produced the mixing) including a green phase believed to be chromian pyroxene. UCLA Image. (b) Cut face of the 450 kg mass of Mont Dieu; six relatively large silicate inclusions are visible on the right side of the face. Wikimedia image.

typically occupy roughly 5–10% of the area of large sections. In some IIE sections the silicates form oriented stringers, apparently a reflection of shear deformation that occurred just before the mass became rigid.

In the Colomera section shown in Fig. 1b silicates are abundant at each end of the slab but uncommon in a broad central band. The high aspect ratios of silicate stringers on the left end suggest that the direction of shear was roughly parallel to the plane of the section whereas on the right end, even though only 25 cm away, aspect ratios are near unity implying either less shear or that the shear plane was roughly perpendicular to the plane of the section.

In addition to silicates, IIE irons commonly contain variable amounts of schreibersite and troilite. Some have very large amounts of FeS; 33 vol% in HOW 88403 (Clarke et al., 1990), 20 vol% in SAH 03505 (D'Orazio et al., 2009) and Prospector Pool (Meteoritical Bull. 94).

Tarahumara (Fig. 3a) shows crystalline silicates including green chromian diopside; the other minerals probably include sodic plagioclase and orthopyroxene reported by Takeda et al. (2003) in a smaller section. The metal records numerous small (2–3 cm) parental gamma regions and kamacite ca. 0.5 mm thick. Cutting the large (430 kg) Mont Dieu specimen revealed a cluster of centimeter-size silicate-

troilite inclusions (Fig. 3b). Investigations of one silicate body showed recognizable chondrules (Van Roosbroek et al., 2015).

An overview of the properties of IIE silicates is given by Bunch et al. (1970). Detailed descriptions of the silicates in additional IIE meteorites are given by Ruzicka et al. (1999), Takeda et al. (2003) and others.

### 3.3. Metal compositional data

In Table 2 mean INAA data for 13 elements in IIE metal are listed; a couple of analyses of Ru and Os are in a footnote. As noted above, we also determine Fe but use it as an internal control of counting geometry. Replicate analyses are listed alphabetically in Table A1 in the Appendix.

As discussed below, it facilitates the discussion to separate the IIE irons into two categories, the main set and the high-Cu (or FeS-rich) set. These are listed separately in Table 2 and are shown with different symbols in the compositional diagrams. Because of its small total mass I could only obtain one INAA sample of NWA 5608; it is listed (and plotted) separately because the data did not yield an unambiguous assignment to either subgroup.

In Table 2 I also list the bulk analysis of the FeS-rich IIE SAH 03505 by D'Orazio et al. (2009). Also listed in Table 2 are two analyses of coarse metal veins from the Portales Valley (PV) H6 chondrite published by Rubin et al. (2001). Because of the relatively large range in compositions both replicates are listed. IIE metal is quite similar in composition to PV vein metal.

Concentrations of 12 elements in IIE metal are plotted against Au in Figs. 4 and 5. The IIEs are divided into three sets: the main set is shown as diamonds, a Cu-rich set as triangles; the ambiguous position of NWA 5608 iron (for which we have only one analysis) is shown as a square. As discussed in more detail below, the members of all three sets are legitimate IIE irons; they are plotted separately to facilitate the discussion.

Also listed in Table 2 and plotted in Figs. 4 and 5 are data for metal veins from the Portales Valley (PV) H6 chondrite (Rubin et al., 2001). The PV means fall within the IIE fields for every element except Co (PV high) and Ga (PV low); we do not have PV data for Ge. The possible significance of the IIE-PV compositional relationships are discussed in the following section.

### 3.4. Stable and radiogenic isotopes

There is now considerable O-isotopic data for IIE irons. Clayton and Mayeda (1996) and McDermott et al. (2015) each report data for 8 IIE meteorites; the only difference in the sample sets is Garhi Yasin (McDermott) and Elga (Clayton). The data sets are shown as histograms in Fig. 6. In each case they are compared with H4–H6 data from the same analytical teams (Clayton et al., 1991; McDermott et al., 2015). These important data sets are discussed in Section 5.

The exciting development of the past decade is that isotopic anomalies are present in numerous elements and that isotopic compositions show different ranges in different groups of meteorites. Non-mass dependent (and, almost certainly, presolar) anomalies are now known in a number of meteorites for Cr, Ti, Ni, Mo and Ru. There are several data for IIE meteorites. Burkhardt et al. (2011) reported Mo isotopic data for metal from Miles and Watson and Trinquier et al. (2007) reported Cr isotopic data for Mont Dieu. Fischer-Gödde et al. (2016) report Ru and Mo isotopic data for the metal from 9 IIE irons and from H5 Portales Valley.

At present there are three main kinds of radiogenic-isotope age data available for IIE irons. Two involve long-lived radionuclides (the $^{87}Rb$–$^{87}Sr$ and the $^{40}K$–$^{40}Ar$ systems) and one involves a short-lived nuclide (the $^{182}Hf$–$^{182}W$ system). Formation ages are discussed in reviews by Bogard et al. (2000)—mainly the $^{40}K$ system and Ruzicka (2014)—mainly the $^{87}Rb$ system. Burnett and Wasserburg (1967) made the important inference that the low (3.8-Ga) Rb–Sr age of Kodaikanal was a formation age but later researchers (e.g., Göpel et al., 1985; Bogard et al., 2000) have concluded that this is an impact-melting age. A key observation is that chondritic materials rather than previously differentiated materials were melted.

Fischer-Gödde et al. (2016) report a wide range in pre-exposure $\varepsilon^{182}W$ values for IIE irons. If interpreted as model formation ages, these span a period from 4 to 28 Ma after CAIs.

## 4. MODELS FOR THE FORMATION OF GROUP IIE METEORITES

Numerous scenarios have been proposed for the formation of the IIE meteorites. I will not review all these models but only discuss the main themes. There is by now general agreement that impacts have played a major role in the formation of the textures and compositions of most IIE irons; I will thus accept the consensus view that impact melts were produced during the formation of all IIE irons.

The first matter to discuss is whether the metal in IIE irons formed by fractional crystallization. This key feature of magmatic irons indicates that they formed as large, slowly cooling melt bodies, almost certainly in asteroidal cores. In the following section we show that there is no evidence of fractional crystallization in group IIE. In Section 7 we discuss evidence indicating differences in fractionation processes between IIE and IAB-MG metal.

Several IIE irons have had their radiogenic isotope systems and their textures disturbed by impacts about 3.6 Ga ago. In the discussion I will focus on the early impacts; if the term "late" is not used, the reader should assume that early impact(s) 4.5–4.6 Ga ago are being discussed. The late impacts will be discussed as an addendum to the primary model.

Various kinds of coarse crystals are found in IIE silicates. These seem to require slow cooling or long-term annealing. The question is whether melt had produced differentiated silicate products before the impacts that produced the IIE meteorites in our collections. Ruzicka (2014) argues for the existence of early silicate melts and refers to these as endogenic (and produced by $^{26}Al$ heating). There seems to be no petrographic way to distinguish early

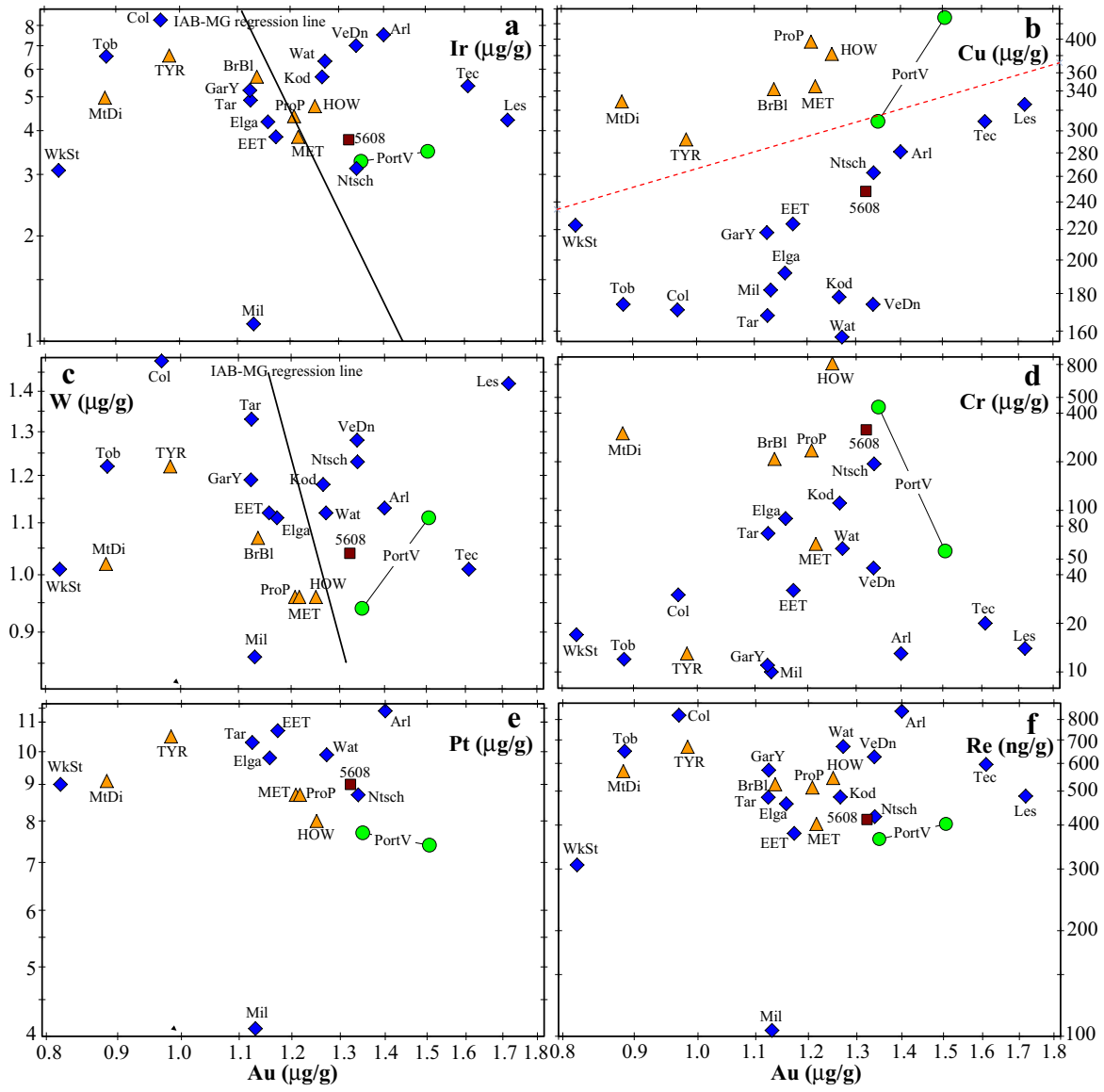


Fig. 4. Log element-log Au diagrams showing concentrations in IIE metal for a) Ir, b) Cu, c) W, d) Cr, e) Pt and Re. Data are also shown for samples of a thick metal vein from the Portales Valley H6 chondrite. Ranges are quite small for all elements, especially if the anomalous IIE Miles is neglected. On the Ir and W diagrams straight lines shows the correlation slopes calculated for the IAB main group; these are much steeper than the ill-defined trends in group IIE, an indication that there were important differences in the formations of the two groups. A subset of Cu-rich (and FeS-rich) meteorites is marginally resolvable in composition relative to typical IIE irons. A dashed line shows the boundary between the Cu-rich set and the normal IIE-set.

melts produced by endogenic heating from those produced by impact heating thus it seems sufficient to divide IIE models into those involving early melts and those that do not. The main issue is whether there are IIE silicate components that require appreciable fractionation processes in melt bodies, or whether all fractionations can be explained by processes occurring in impact melts that cooled relatively fast at high temperatures but were annealed for long periods at. the metamorphic temperatures responsible for coarse metallic structures.

A last issue is whether the metal in IIE irons originated together with the silicates on the same asteroid (e.g., Wasson and Wang, 1986) or whether separate asteroids produced the metal and the silicates (e.g., Ruzicka, 2014).

## 5. DISCUSSION: COMPOSITION AND CHARACTER OF METAL IN IIE IRONS AND PORTALES VALLEY

The simplest IIE formation model is that the metal and silicate were both produced by melting and metal–silicate separation in a single chondritic asteroid. However, as noted by Ruzicka (2014), some researchers have inferred that the IIE metal component originated on a second asteroid that had already differentiated. This conclusion is not

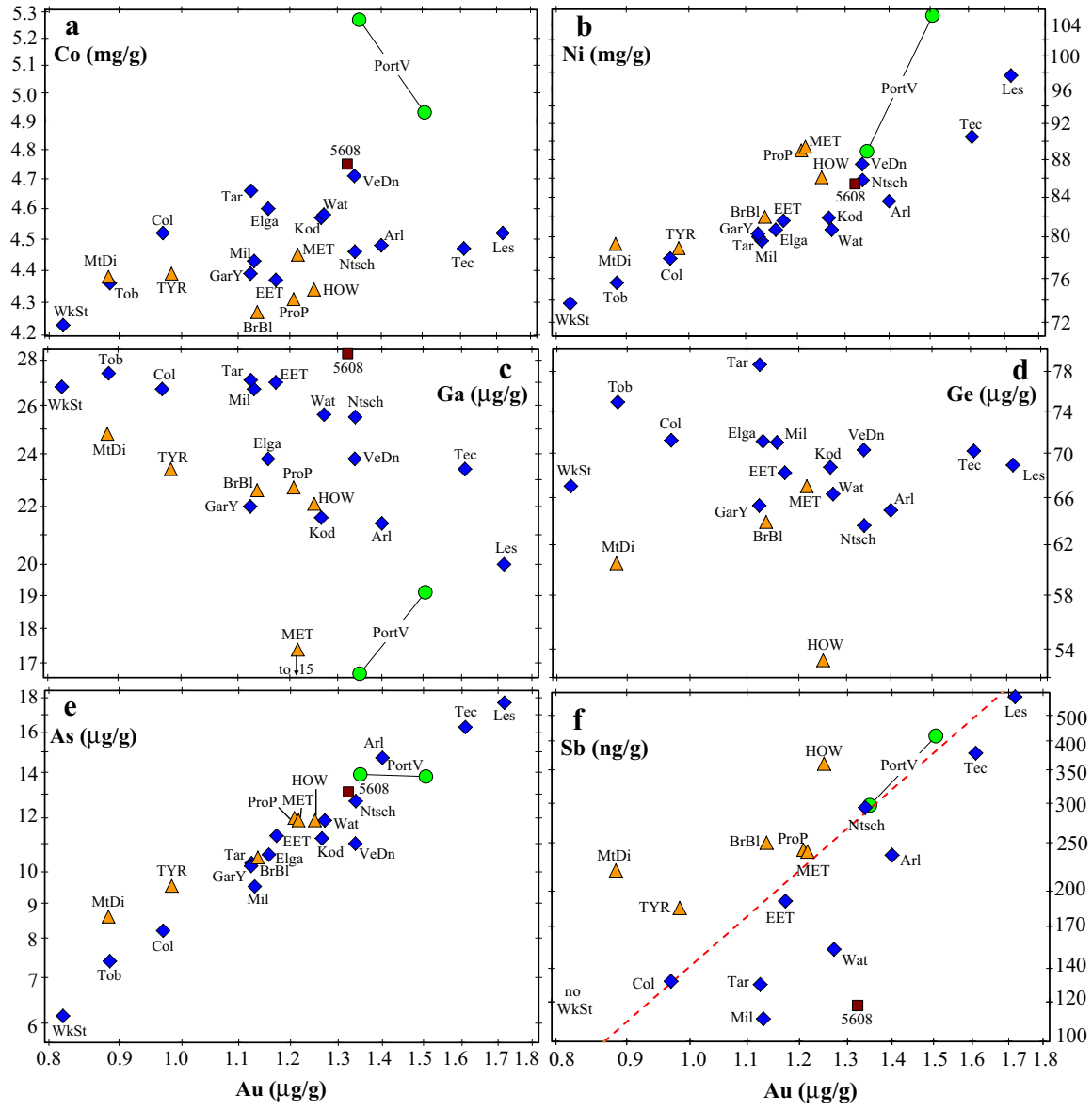


Fig. 5. Log element-log Au diagrams showing concentrations in IIE metal for a) Co, b) Ni, c) Ga, d) Ge, e) As and f) Sb. Relative to typical IIE irons the Cu-rich subset tends to have lower Co, Ga and Ge in the metal and higher Ni, As and Sb. A dashed line shows the boundary between the Cu-rich and the common set on the Sb–Au diagram. These differences may reflect low-temperature partitioning between FeS and kamacite but detailed data on FeS are not available. On most of these diagrams and those in Fig. 4 there are three loose compositional clusters: Elga and EET, Kod and Wat, and HOW 88403, MET 00428 and ProP.

supported by the metal compositions discussed below that show an absence of fractional crystallization effects in the IIE irons and show chemical and isotopic compositions consistent with those in Netschaevo and other primitive silicates (and, generally, in ordinary chondrites).

As mentioned above and discussed in more detail in Section 10, the isotopic compositions of Mo and Ru vary among the chondrites. The recent data of Fischer-Gödde et al. (2016) show that IIE metal has the same Mo and Ru isotopic compositions as ordinary chondrites. Because of this and the absence of fractional crystallization effects, I will focus on models calling for silicates and metal to be produced on a single asteroid. If the heat was provided by an impact, then some of the IIE materials may have originated on the projectile asteroid but, as discussed later, compositional signatures of the impactor have not been resolved.

As can be seen in Figs. 4 and 5, most elements show small ranges in IIE. The largest range is observed in Cr (Fig. 4d), but most of the Cr in IIE irons having concentrations >∼200 µg/g appears to be present in scattered chromite grains rather than metal. Although chromite was probably a liquidus phase, the small scatter between most replicate pairs indicates a small grain size and uniform

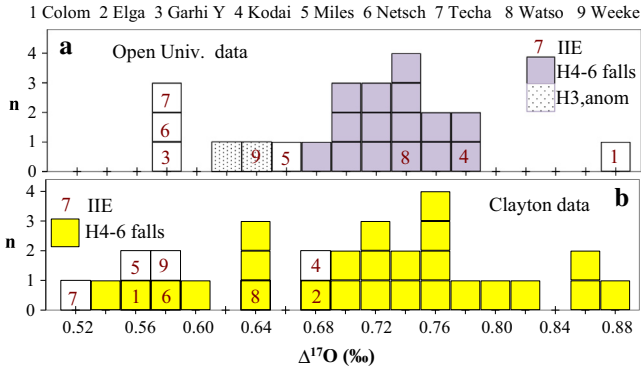


Fig. 6. Distribution of $\Delta^{17}O$ values in IIE silicates (a) reported by McDermott et al. (2015) and (b) reported by Clayton and Mayeda (1996). These are superposed on shaded histograms of H4–H6 chondrites, reported by McDermott et al. (2015) in part a and by Clayton et al. (1991) in part b. Shown stippled are McDermott et al. data for H3 Dhajala and for the impact altered Rose City H chondrite, both of which plot lower than the "gaussian" H4–H6 peak. The IIE points have a central Arabic numeral and fall either on shaded or unshaded squares. Three IIEs with chondrule-bearing silicates plot at values much low than the McDermott et al. (2015) H4–H6 peak. Errors are larger in the Clayton data set but the mean data in the two sets are in general agreement. The discrepancy between the Colomera values is outside expected experimental uncertainties. None of the analyzed meteorites belong to the Cu-rich set of IIE irons.

initial distribution; larger grains can lead to large sampling variations. Data in the accompanying online materials show that replicate Cr values in IIE irons can be quite different (e.g., Mont Dieu replicate values are 520 and 83 μg/g, those in Elga are 138 and 31 μg/g).

It was noted that, if Miles is treated as anomalous, refractory siderophile concentrations vary by factors of 2 to 3. Large, factors of ~ 3, ranges are also observed for As (Fig. 5e) and Sb (Fig. 5f) and that of Au is a factor of 2. Of these, the most volatile is Sb and it may have been somewhat mobile during impact heating. The large Au range is surprising because the range is only a factor of 1.2 in IAB-MG. Possible mechanisms for producing the larger Au range in IIE are that there may be different fractions of the nebular host phase(s) in different batches of melt in different portions of the impact heated materials; in contrast, the IAB-MG irons seem to have formed from a single large, flowing body of melt, which resulted in some mixing. And, as discussed in Section 6.2, the IIE Au range might instead also reflect compositional differences between melt produced from the target asteroid and melt produced from the projectile.

In magmatic groups the supercompatible element Ir ranges are large and there is always a steeply negative slope (the result of fractional crystallization) on Ir–Au diagrams; the lowest Ir abundances are far lower than those in chondrites. In group IIE there is a hint of a negative correlation between Ir and Au but all Ir/Fe ratios are in the general chondritic range. Like Ir, the other refractory siderophile elements Re (Fig. 4f), W (Fig. 4c) and Pt (Fig. 4e; we are missing Pt for most IIE irons) are super-compatible in the magmatic groups but show negligible correlations with Au in group IIE. The absence of trends is consistent with an impact origin but differences with IAB trends warrant a more detailed discussion.

In IAB-MG, the other large non-magmatic group, there are well-defined negative trends between Ir and Au and between W and Au; we plot Ir–Au and W–Au data in Fig. 7. The lines show mean slopes obtained by assigning equal relative errors to the *X* and *Y* variables. Lines with these IAB-MG slopes are shown on the Ir–Au and W–Au plots of group IIE data (Fig. 4a and c). Possible reasons for these very different IIE and IAB-MG Ir–Au trends are discussed in Section 8.

The six IIE irons with high Cu were given different symbols to call attention to some weak but probably significant trends in the data. As shown in Table 2, these six irons also have high FeS contents. A tendency of the two IIE sets to separate is also observed in the elements plotted on Fig. 5. Over the same range in Au the concentrations of Ni (Fig. 5b), As (Fig. 5e) and Sb (4f) are higher and the concentrations of Co (Fig. 5a, Ga (Fig. 5c) and Ge (Fig. 5d) are lower than in the main set.

In Section 7.3 and Appendix B I discuss some factors (e.g., high FeS in the high-Cu irons) that may be related to these differences. At this time the differences seem to be too small to warrant the designation of these Cu-rich irons as "anomalous". However, these minor differences should be considered when searching for correlations of other properties within sets of IIE elemental data.

## 6. DISCUSSION: BULK DATA ON IIE IRONS, H CHONDRITES, NETSCHAEVO AND PORTALES VALLEY

It seems likely that all (or nearly all) the IIE irons formed on the same asteroid. Their compositions are so similar it would be surprising if a sizable fraction (e.g., the ones with formation ages ~3.6 Ga) were from a separate asteroid. This is therefore my working assumption.

There is no doubt that the IIE meteorites are closely related to the H and HH ordinary chondrites (OC). The first clear link was the similarity in metal compositions in common IIE irons and HH Netschaevo (Wasson, 1970). Olsen and Jarosewich (1971) noted that the silicate blocks in Netschaevo are samples of a metamorphosed chondrite

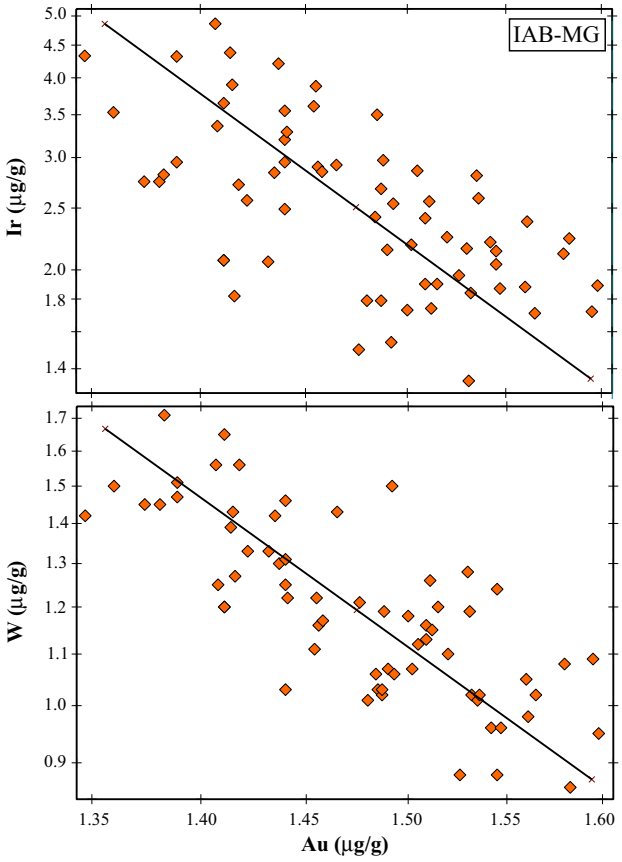


Fig. 7. In contrast to the ill-defined trends in IIE, Ir–Au and W–Au diagrams for the main group of IAB show strong negative trends. Lines with the same slopes as the regression lines shown here are shown on Figs. 4a and 4c. This difference in behavior is interpreted to mean that the IAB melts were hot enough to flow moderate distances while crystallizing whereas, after the impact melting event, the IIE melts solidified too quickly to permit even the limited degree of fractionation observed in IAB-MG.

similar to H chondrites but more reduced (Fa14 in olivine, below the H-group range of Fa16 to Fa20).

Bild and Wasson (1977) obtained trace element data for chondritic silicate blocks in Netschaevo and found that siderophile element contents are higher than those in H chondrites and that Netschaevo could reasonably be classified as a new (HH) class of OC. Müller et al. (1971) had reported trace-element data for OC and interpreted the trends to indicate that the three groups (H, L and LL) are best understood as an incompletely sampled continuous-fractionation sequence, thus Netschaevo represented the first known member of the OC fractionation sequence that is more reduced and siderophile-rich than the H chondrites.

### 6.1. Oxygen isotopes in IIE meteorites and H chondrites

Non-mass-dependent fractionations of O isotopes provide an excellent tool for assessing genetic relationships among meteorites. Studies of IIE meteorites and H chondrites have been published by Clayton et al. (1983, 1991) and by Clayton and Mayeda (1996). Data for both IIE meteorites and H-chondrites were published by McDermott et al. (2015). These two data sets are compared in Fig. 6. The Van Roosbroek et al. (2015) Mont Dieu $\Delta^{17}O$ value (0.7‰) is from another laboratory and not included in Fig. 6.

The lower histogram compares the IIE $\Delta^{17}O$ data of Clayton and Mayeda (1996) with values reported by Clayton et al. (1991) for H4–H6 chondrite falls. The mean $\Delta^{17}O$ of IIE irons (0.59‰) is appreciably lower than that in H falls (0.71‰) but there is considerable overlap; all IIE values are below the median H4–H6 value of 0.72.

The upper diagram in Fig. 6 shows IIE and H data reported by McDermott et al. (2015); it is labelled Open Univ. data. These authors gathered this more precise set of O-isotope data using laser fluorination; most samples were analyzed more than once. If one ignores the anomalously high value (0.88‰) of Colomera, their range in IIE $\Delta^{17}O$ values (0.58 to 0.78‰) is slightly larger than that (0.62–0.78‰) reported by Clayton and Mayeda (1996). The H4–H6 chondrite range of McDermott et al. (2015) is small and roughly gaussian in shape if the low values of H3 Dhajala and the heavily impact-altered Rose City (Rubin, 1995) are neglected (these squares are shown stippled in Fig. 6).

In the Open Univ. data set 2 of the 8 IIE values fall within the H4–H6 fields and 3 are lower than all the H including the anomalous H3 Dhajala; Colomera is about 3$\sigma$ above the centroid. The difference between the McDermott and Clayton Colomera $\Delta^{17}O$ values is outside the range expected from laboratory precisions; more investigation of this seemingly heterogeneous meteorite is needed.

McDermott et al. (2015) suggested that the wide range of their IIE results could be formed by the impact melting of unequilibrated H chondrites consisting of components having a wide range in $\Delta^{17}O$. This view is supported by studies by Clayton et al. (1991) of milligram-size chondrules from unequilibrated OC that commonly yielded much scatter and numerous values outside the fields defined by equilibrated members of these groups. As discussed in Section 10.2, this variability reduces the usefulness of $\Delta^{17}O$ as a taxonomic tool.

### 6.2. Siderophile abundance ratios in IIE meteorites and in H and L chondrites

Fig. 8 compares mean Au-normalized elemental abundances of IIE metal with H-chondrite siderophile data from Kallemeyn et al. (1989) for H4, H5 and H6 observed falls. Only the anomalous (low-Ir) IIE Miles is excluded from the IIE mean (and its inclusion would result in only minor changes). Kallemeyn et al. (1989) did not determine Cu, W and Re in H chondrites; for these the mean concentrations from the review paper by Wasson and Kallemeyn (1988) were used.

Inspection of Fig. 8 shows that, relative to H chondrites, IIE irons have higher abundance ratios of the refractory siderophiles Re, Ir and W and lower abundance ratios of the volatile siderophiles Cu, Ga and Sb, inconsistent with models calling for formation from H-chondrite-like precursors. H-like ratios are observed for the common elements Ni and Co and the slightly volatile As and Au. Although some loss of Ga, Sb and Cu may have occurred during impact event(s) believed to have melted the IIE silicates and metal, the high Sb and As contents of Portales Valley impact-produced metal suggest that the fraction lost was minor (perhaps 10% or less). The low Cu abundance ratio probably also reflects the ill-understood process (perhaps partitioning into a largely unsampled phase such as FeS-rich materials) that causes mean Cu/Au ratios in irons to be several times lower than chondritic ratios.

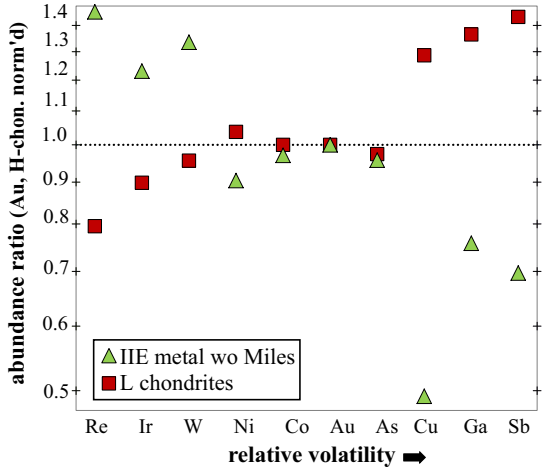


Fig. 8. IIE elemental abundances normalized to Au and H chondrites decrease with decreasing 50% condensation temperature (and increasing degree of volatility). This is opposite to that observed with L chondrite abundances, which increase with increasing volatility. These fractionations seem to have been produced in the solar nebula.

Also plotted in Fig. 8 are H- and Au-normalized abundance ratios in L chondrites. The L trend is the opposite of the IIE trend. Granted that the three groups are ordinary chondrites (H and L) or the products of impact melting of ordinary chondrites (IIE), the trends in Fig. 8 strongly support the idea that IIE metal formed from chondritic materials more enriched in refractory siderophiles and more depleted in volatile siderophiles than H chondrites. This is consistent with an "HH" origin. The same trends were observed by Bild and Wasson (1977) in Netschaevo.

Portales Valley (PV) is an H chondrite that, in some regions, hosts broad (up to 2 cm) metal veins that are clearly the product of impact melting (e.g., Kring et al., 1999; Rubin et al., 2001; Ruzicka et al., 2005). As noted above, the compositions of the PV metal veins (filled circles in Figs. 4 and 5) are closely related to those observed in IIE metal; the exceptions are Co (PV slightly higher) and Ga (PV slightly lower). The difference in Co may reflect a difference between H and HH; the low Ga may mainly indicate that some Ga was in a phase (e.g., an oxide) that did not contribute to the metallic melt during the brief impact-melting event. This is the inverse of a suggestion by Ruzicka et al. (2005) that, after the melting event, conditions became more oxidizing and Ga was lost from the metal by diffusional exchange with silicates.

## 7. DISCUSSION: MODELS TO EXPLAIN THE FORMATION OF IIE IRONS AND THEIR SILICATES

The IIE metal and most of their silicates experienced melting; my working model is that the main source of heat was impacts. Some heat was also produced by the decay of 720-ka $^{26}Al$. Kita and Ushikubo (2012) determined $^{26}Al/^{27}Al$ ratios in about 20 LL Semarkona chondrules; it is probable that HH and LL ratios were similar. The chondrules with the lowest well-determined ratios formed last and thus give the maximum ratios available for heating the OC asteroids. From Fig. 5 of Kita and Ushikubo (2012) it appears that the appropriate value is about $5{\cdot}10^{-6}$.

However, even in a well-insulated body, this ratio provided only enough energy to raise the temperature of HH material about 1000–1100 K (see the general discussion in Schramm et al., 1970, and Kunihiro et al., 2004) provided the chondrite body formed a small fraction of a $^{26}Al$ halflife after the formation of the youngest chondrules. If the initial temperature was 200 K, this ratio is only marginally enough to melt the Fe–FeS eutectic at about 1250 K.

It thus seems clear that impacts were the main source of the heat needed to bring solids to the melting temperature and supply the necessary latent heat. The efficiency of

converting impact velocity to heat increases with porosity, and it may be that the target was an uncompacted chondritic asteroid. Impact may have even been the heat source for magmatic irons; Wasson et al. (2006) proposed that impacts were responsible for melting and reducing L-LL materials in order to produce the IVA magma.

Although some authors (e.g., Ruzicka, 2014) have assumed that higher $^{26}Al/^{27}Al$ ratios were present in early-formed chondrites that are not in our collections, the young formation ages (4–28 Ma after CAIs) inferred from $\epsilon^{182}W$ values in IIE metal by Fischer-Gödde et al. (2016) imply metal silicate formation too late for the dominant heat source to have been $^{26}Al$.

### 7.1. The Wasson–Kallemeyn model for forming nonmagmatic group IAB-MG; application to IIE formation

The properties of IIE meteorites differ in important ways from those in the larger nonmagmatic group IAB-MG. The IIEs have more processed silicates and record less differentiation in the metal.

In the nonmagmatic irons, because of high cooling rates following impact melting, equilibrium was only achieved between the crystallizing solid and the adjacent melt layer; there was insufficient stirring to keep the residual magma mixed. As a result, ideal fractional crystallization (as observed in the large magmatic groups IIAB and IIIAB) could not occur; the high degrees of fractionation of Ir and similar supercompatible siderophiles were not produced.

This is one of the arguments indicating that these groups did not originate in a slowly cooling asteroidal core. An equally important argument is the presence of trapped silicates in the metal of both nonmagmatic groups. During the slow cooling required for fractional crystallization silicates will buoyantly separate from melts during timescales orders of magnitude shorter than those required for fractional crystallization.

Wasson and Kallemeyn (2002) proposed a simple model to explain the solidification of IAB melts following impact melting. After formation by an impact near the surface of the asteroid, residual silicates separated from the metallic melt as a result of upwards-buoyancy forces and the metallic melt started to trickle down through the underlying cool, chondritic rubble. The heat transferred to the solids by these melts caused thermal metamorphism of chondritic clasts but only minor amounts of silicate melting.

The metallic melt layer next to the rubble cooled by conduction, and crystallized. This led to a small depletion of compatibles and enrichment of incompatibles in the remaining melt, but complete mixing of the liquid (as required for fractional crystallization) was not achieved. In IAB-MG where (neglecting a few irons with very low Ir contents (including Morasko) that seem not to have formed from the same body of melt) the total range in Ir is by a factor of about 4.5 and Ir–Au diagrams show a significant negative trend (Fig. 7). Thus some fractionation occurred, but far less than in IIAB or IIIAB. In IIE (neglecting the outlier Miles) the range is 2.6, appreciably smaller than in IAB-MG and there is no significant (negative or positive) Ir–Au trend. Thus, although the metal in the two groups formed by impact melting, the evolutionary processes differed in important details.

Related is the difference in the formation of the common silicates. In IIE these are differentiated, in IAB almost exclusively subchondritic. It is clear that the differentiated silicates experienced much higher temperatures than the common IAB silicates. This suggests that IIE precursor silicates were sited near ground zero where the projectile hit the target and temperatures were the highest. There has been some melt–solid separation in IAB but regions in which all coarse silicates are differentiated have not been recognized among known IAB-MG meteorites.

Thus, compared to IAB, IIE meteorites generally record higher temperatures in the common silicates and their metal shows a lesser degree of fractionation implying that it cooled to solidus temperatures more rapidly. Rough estimates suggest that the minimum temperature necessary to produce appreciable melting of albitic silicates (and a small fraction of mafic minerals) was about 1500 K. At this temperature most of the metal would not melt.

Although one can melt the Fe–FeS eutectic at 1260 K, the dominant component is FeS; 88% of the mass is FeS and only 12% is metal. Even the most FeS-rich IIE metal has a much higher melting temperature. Some IIE irons have FeS contents several times lower; Buchwald (1975) found no FeS in Arlington, implying a melting temperature of ~1750 K at 100 mg/g Ni (Brandes and Brook, 1998).

Jarosewich (1990) reported the FeS content of Netschaevo silicates to be 37 mg/g. thus the melt fraction of the whole-rock is only 42 mg/g at the eutectic temperature. If all the metal (213 mg/g) in Netschaevo melted this would lead to a melting temperature of about 1660 K, about 400 K higher than the eutectic temperature. According to the Fe–S phase diagram in Brandes and Brook (1998), at 1500 K the FeS fraction is 70% and the Fe (metal) fraction is 30%. Replacing about 8% of the iron with Ni would slightly increase the metal fraction at 1500 K. I conclude that at the time of formation, the temperature of the metallic melt was >1600 K.

The viscosity would have been relatively low. Even a high S/Fe atomic ratio of 0.28 has a viscosity of about 0.002 Pa s at ~1750 K (Terasaki et al., 2006) and the IIE melt probably had a S/Fe ratio about 5× lower resulting in a similarly low viscosity at 1700 K. Stoke's law calculations show that a 0.1-mm-diameter silicate sphere will move 100 m through molten metal in about 10 days at the surface of chondritic body with a radius of 100 km and a density of 3.6 g $cm^{-3}$. It is probable that, immediately after the impact, re-accreted ejecta covered larger melt bodies with enough low-conductivity porous regolith to retain high temperatures for periods this long. This seems the most probable scenario for the seven or more IIE irons that appear not to contain silicates.

Those that do contain silicates must have cooled faster. My working model is that the chondritic silicate blocks (e.g., Netschaevo) were engulfed by melt flowing downward into the rubble pile asteroid, the same model invoked to account for IAB-MG meteorites. An interesting complication is that Netschaevo also contains centimeter-size

impact-melt clasts interpreted to be the result of a second impact event that also reset the $^{39}Ar$–$^{40}Ar$ age to ca. 3.6 Ga (Van Roosbroek et al., 2016).

Most of the other IIEs (and especially those preserving glass) also had to chill quickly. I suggest that these formed in small melt bodies that were able to cool much more rapidly by heat conduction into nearby cooler materials.

Some silicates may also have been introduced during secondary impact events. As pointed out by Ruzicka (2014) and others, the presence of glass and fine octahedral patterns in the IIE irons having low $^{39}Ar$–$^{40}Ar$ ages is a strong indication of production in secondary impact events with the resulting samples cooling quickly, presumably because the heated volumes were small and able to quickly lose their heat into local materials.

As discussed above in connection with Fig. 8, mean abundance ratios in IIE metal are consistent with formation from HH chondrites, a kind of OC more reduced and siderophile-rich than H chondrites. The roughly chondritic siderophile compositions of IIE irons suggests that most of the carriers of common and volatile siderophiles melted, became incorporated into the melt, and chilled too quickly to allow appreciable fractionation between compatible and incompatible siderophiles.

### 7.2. Compositional evidence of the projectile?

Impact models predict that a minor fraction of the siderophile elements will have been contributed by the projectile. The fraction will have depended on the nature of the projectile, its collision velocity, the porosity of the target and projectile and, because of these, the fraction of the projectile that vaporized and escaped the system. Asteroid impact velocities are much lower than those on the Earth or the Moon. In the inner Asteroid Belt mean interobject velocities are about 5 km $s^{-1}$ at present but higher velocities were present 4.5 Ga ago when some projectiles had semimajor axes >10 AU and there is self-selection-effect for the higher velocity (say 10 km $s^{-1}$) projectiles to be the ones that produce melts. At 10 km $s^{-1}$ the projectile contribution is probably a few per cent but, for the reasons just listed, uncertainties are large.

If projectile siderophiles had distinctly different element-Au ratios compared to those in the target asteroid then one should see an array connecting the two end components. If the slope of this array were distinctly different from the main IIE slope, we might recognize it as a trend line intersecting the main trend line. I see no evidence for this in the data in Figs. 4 and 5. Perhaps there is a large projectile component in Miles which accounts for its anomalously low contents of Ir, Pt and Re. If the impactor had a composition similar to the target, its presence would be impossible to resolve. And, if the projectile fraction was <5%, the scatter in the data makes it difficult to resolve the projectile component unless the composition was very different from that of the target.

On the other hand, the range in Au contents in IIE is much larger than that in IAB-MG (factor of 2 range in IIE, factor of 1.2 range in IAB-MG). Perhaps this range is the result of different Au/Fe ratios in the target and projectile. If this is the explanation, then it may be possible to confirm this interpretation by comparing the isotopic composition of siderophiles such as Mo or Ru in low-Au irons with those in high-Au irons. However, impact effects can vary widely on small (several centimeter) scales; the large range in Au may reflect different degrees of melting of several Au carrier phases in the target precursor materials.

### 7.3. Possible origin of high-Cu set

Wasson (1999) discussed the role of melt trapping during the formation of the IIIAB magmatic group. During fractional crystallization the melt and the crystallizing solid are always in equilibrium. If a mechanical event (perhaps caused by the detachment of a solid slab from the ceiling of the magma chamber and its settling onto the floor) the composition of the resulting meteorite (after mixing by diffusion) will lie along a mixing line between these two compositions. An example of this was described in the Cape York irons by Esbensen et al. (1982); there is a mean difference of about a factor of 2 in Ir and Au contents between the Cape York Savik mass (having a low content of trapped melt) and the Agpalilik mass (having a high content of trapped melt). To produce the evidence or rapid mixing and cooling provided by the FeS and silicate textures in the IIE irons it seems clear that the mean temperature was well above that of the eutectic.

Before discussing the formation of group IIE in more detail I want to examine possible explanations for differences in FeS contents among IIE irons. In Section 4 it was noted that elemental concentrations in the high-Cu IIE set tend to plot above or below the trends through the main set; on the Cu–Au diagram the two sets can be separated by a straight line (Fig. 4b). It simplifies this discussion to first explore possible explanations for the high Cu concentrations in IIE irons. All six high-Cu meteorites (Barranca Blanca, HOW, MET, Mont Dieu (Fig. 3b), Prospector Pool (Fig. 2b), and TYR 05181) have relatively high (>20 mg/g S) FeS contents. SAH 03505, another high-FeS IIE iron studied by D'Orazio et al. (2009), also has a high Cu content (341 μg/g). As discussed above, on the Cu–Au diagram (Fig. 4b) the main set of IIE irons shows a marginal positive trend but the scatter is too large to even confirm the sign of the trend.

Several factors must be considered in order to evaluate processes that could explain the compositional differences between the high-Cu set and the main set of IIE irons: (a) Cu may have been present in different phases in the nebular precursors melted to produce IIE metal; (b) because Cu is more siderophile at higher temperatures, rapid chilling of an impact generated metallic melt (for example, if it was intruded into cooler silicates) could lead to higher concentrations in the solid metal; and (c) if Cu metal is formed (e.g., as a result of nucleation on impact-generated defects) diffusional draining of Cu from Fe–Ni metal into Cu metal could occur at subsolidus temperatures. These are discussed in some detail in the online materials.

The vagaries of impact heating and Cu nucleation may play important roles in determining whether the metal of a IIE iron has a high or low Cu content, but the dominant

factor seems to have been the association of Cu with S-rich melts.

## 8. DISCUSSION: IMPACT MELTING AND THE SIGNIFICANCE OF DIFFERENCES BETWEEN IIE AND IAB-MG

The cosmochemical community has been reluctant to seriously consider impacts as a source of kilometer-scale asteroidal melting. In large part this is attributable to the Keil et al. (1997) paper which argued that impacts could not produce enough heat. There are, however, two problems with that paper which greatly reduce the strength of this conclusion: (1) the discussion of impact generation of melt is mainly based on the study of terrestrial craters in which the targets have very low porosity whereas conversion of kinetic energy to heat scales roughly proportional to the porosity of the target. Impacts into high-porosity asteroids (and the first planetesimals had extremely high porosities) would be much more efficient at converting kinetic energy to heat (see discussion in Section 8). (2) The Keil et al. paper only discussed global heating whereas the melts required to produce the non-magmatic meteorites could have been tiny fractions of the asteroid volume.

In addition, radiogenic heat sources (at present, $^{26}$Al decay is the only one seriously considered because initial $^{60}$Fe/$^{56}$Fe ratios were so low (Tang and Dauphas, 2015; Telus et al., 2016) release their heat at a far slower rate than impacts and this leads to a very different thermal evolution of the asteroid. Impacts produce melt that can be quickly chilled by flowing onto cold debris. Temperatures of magmas generated by radionuclide decay increase so slowly that melt becomes gravitationally unstable and separates already at low degrees (perhaps 20%) of melting with the result that basaltic liquids separate upwards and S-rich metallic melts move downwards in the asteroid. For this process to have been important for IIE formation requires very special circumstances (such as correctly-timed impacts) to stop this process at just the right time while melt and mafic silicates are still in contact with each other. This alone makes this scenario implausible.

Group IAB-MG is the largest non-magmatic group and group IIE the second largest. Although the metal in both these groups did not form by the efficient fractional crystallization that is so clearly evident in the large magmatic groups IIAB (Wasson et al., 2007), IIIAB (Wasson, 1999) and IVA (Wasson and Richardson, 2001), they also differ from each other in their metal trends and in their silicate compositions and morphologies. It is clear that the nature of these impacts and their consequences were quite different in the two source asteroids.

Group IAB-MG has many members and compositional trends are thus well defined. There are far fewer IIE irons and a moderate amount of scatter although some of the latter is a stochastic effect related to the very low ranges for most elements. For example, with the exception of Miles, the total range of Ir in IIE is only a factor of 2.6, only marginally larger than the Au range. And, as discussed above, the Au range is a factor of 2 whereas that in IAB-MG is only by a factor of 1.2.

The more massive silicate clasts in IAB are close to chondritic in chemical and mineralogical composition; they commonly consist of angular fragments. In contrast, the common silicates in group IIE are rich in plagioclase/glass (Ruzicka, 2014; McDermott et al., 2015) and have globular shapes that imply that they were largely or completely molten; less common IIE silicates are chondritic or subchondritic and fragmental in shape.

In their study of IAB-MG metal Wasson and Kallemeyn (2002) suggested that the minor degree of igneous fractionation could best be understood to be the result of crystal fractionation of a metallic melt crystallizing as it flowed downward through a rubble-pile asteroid and exchanged heat with the cooler chondritic blocks that it encountered. This model offers a simple explanation for the chondrite compositions of IAB silicates; they are relatively unaltered fragments engulfed by this downward flowing melt. The primitive chondritic fragments are examples of the kinds of chondritic materials that were melted by the inferred impact but were situated outside the zone where extensive (>30%) melting occurred.

In contrast, the typical IIE silicates consist of a low-melting fraction of chondritic materials. Most have high contents of albitic plagioclase and low contents of mafic minerals compared to chondrites. There is one example of an K-feldspar-rich clast 11 cm long (Wasserburg et al., 1968; Takeda et al., 2003) in Colomera which requires a more complex explanation. Because the Na/K weight ratio in OC materials is about 8.5 (Wasson and Kallemeyn, 1988), it is necessary to enrich K in order to produce K-rich plagioclase; the most probable process would seem to be separation of (more volatile) K from Na during vapor transport (the natural equivalent of a fractionation column). To achieve such separation seems to require that the oligoclase-rich sample was located quite far (as a guess,>10 m) from the point where the vaporization occurred.

It thus appears plausible that the albite-rich inclusions are representative of the primary melt products from the impact or impacts that produced the IIE meteorites with the oligoclase-rich samples being appreciably more evolved. However, we have few samples of the (more abundant) mafic counterparts of the plagioclase-rich samples, and thus, as in IAB-MG, we do not have complete samples of the (post-impact) target materials (although the most primitive of the chondritic clasts appear to be metamorphosed samples of the preimpact target). As proposed for IAB-MG, these may be local materials well away from ground zero that were engulfed by the metallic melt.

Many impact-altered chondrites have thin veins of metal or FeS or plagioclase and other silicate phases. This raises the question of whether the plagioclase-rich globules in IIE irons such as Weekeroo or Miles could have been extracted as mobile components from chondritic materials leaving behind residues such as Watson. The problem with this scenario is that the bulk of the material in the IIE meteorites is metal, and it seems clear that the extraction of the metal could not have occurred from chondritic blocks that only lost small amounts of low-temperature melts (including "metallic" melts having high FeS contents). I conclude

that the silicates in Watson are not survivors that were present at ground zero; they were probably sited only slightly closer to ground zero than Netschaevo.

## 9. PRIMITIVE CHONDRITIC MATERIALS, POROSITY AND IMPACT MELTING

It is well understood that the efficiency of conversion of impact kinetic energy to heat (H) increases roughly linearly with porosity. In the equation: $H \propto P \cdot \Delta V$, $P$ is the pressure and $\Delta V$ is the fractional change in the volume (which can be set equal to the porosity).

Modeling studies and laboratory experiments show that, during formation of the first planetesimals from millimeter-size chondrules and micrometer-size fines, porosities were very high (Blum and Wurm, 2008). The minimum porosity at this stage was 50% and it may have been as high as 90%. The chondritic meteorites that fall have porosities of 10–15%. These low porosities cannot be achieved by gravitational compression in small ($r < 100$ km) asteroids; almost certainly they are produced by impact compaction (and the materials that never got compacted aren't tough enough to make it through the Earth's atmosphere to fall as meteorites).

Before the onset of impact compaction all the materials on the asteroid were primitive, unmetamorphosed nebular materials. They recorded chondrule-to-chondrule variations in composition (e.g., FeO/(FeO + MgO) ratios in silicates) as well as differences in isotopic composition. However, if centimeter-size portions of these nebular materials were well mixed (in the lab using a mortar and pestle, in a closed-system asteroid by melting or thermal metamorphism), these variations would be largely leveled out. If the asteroid were not a closed system, then losing or adding components could affect some properties, in particular the O-isotopic composition. For example, in OC such as LL3.0 Semarkona, some phases show high $\Delta^{17}O$ values that have been attributed to interaction with $H_2O$ having $\Delta^{17}O$ of $\sim$+7‰ (Choi et al., 1998).

Impacts produce a range of temperatures. At the projectile-target interface temperatures reach very high values, high enough to vaporize magnesian silicates. The documentable temperatures in IIE meteorites are much lower. In meteorites such as Prospector Pool (Fig. 3a) that contain $\sim$50 mg/g S we know from the Fe–FeS phase diagram that the metallic melt had a minimum $T$ of $\sim$1700 K (Brandes and Brook, 1998). If the impact melt was near the surface of the asteroid, the maximum temperature cannot have been much higher without extensive loss of S and other volatiles associated with convection and outgassing of the relatively low-viscosity fluid; in the presence of metallic Fe and in the absence of appreciable $H_2S$ or $S_2$ pressure, FeS vaporizes at about 700 K.

## 10. ISOTOPIC EVIDENCE REGARDING THE PARENTAL MATERIALS OF IIE METEORITES

Our Earthly sample of asteroidal materials appears to be far from complete. Almost all of our meteorite groups (5 or more members) come from twenty or so asteroids and those that appear to be from other asteroids are often impact altered including the possibility of mixing diverse materials that consist of or were derived from very different kinds of primitive materials (i.e., materials formed at different times or places or both in the solar nebula). There is no reason to doubt that other kinds of chondritic materials formed in the solar nebula. In the case of the OC we know the properties of H, L and LL chondrites so well that we can make plausible extrapolations to infer the properties of an HH material more reduced and metal-rich than the H chondrites. Bild and Wasson (1977) argued that Netschaevo is best classified an HH chondrite.

### 10.1. Anomalies measured in $\varepsilon^{54}$Cr, $\varepsilon^{97}$Mo, $\varepsilon^{100}$Ru and $\varepsilon^{182}$W as measures of genetic relatedness

Since several decades O-isotopes have been used to infer links between differentiated meteorites and possible primitive precursors. During the past decade it has been shown that non-mass-dependent differences in other isotopic systems offer the same kind of taxonomic information; here I limit the discussion to anomalies in $^{54}$Cr, $^{97}$Mo, and $^{100}$Ru. These elements are siderophile (Mo and Ru) or were appreciably siderophile when the metal was molten (Cr) which has the advantage in IIE meteorites that they integrate over larger masses of well mixed materials than do the silicates. These isotopic systems offer the possibility of assessing the degree of precursor (i.e., projectile and target) mixing during the formation of IIE meteorites.

In iron-meteorite metal cosmic-ray effects make it difficult to study $\varepsilon^{54}$Cr variations but there is a relatively large set of data obtained by the study of chromite in which cosmic-ray effects are negligible compared to normal errors. Unfortunately there is only one good IIE $\varepsilon^{54}$Cr datum; Trinquier et al. (2007) reported a range in $\varepsilon^{54}$Cr in 6 OC from $-0.37$ to $-0.48$ and a similar value in chromite from IIE Mont Dieu of $-0.59 \pm 0.13$. The OC data show slightly lower $\varepsilon^{54}$Cr in H and L than in LL suggesting that HH $\varepsilon^{54}$Cr is still lower; however, there are too few samples to be confident that this is a significant trend. Thus the IIE $\varepsilon^{54}$Cr value is consistent with derivation of IIE from materials within the OC range but there is too much scatter to support a claim of a close relationship between IIE meteorites and HH chondrites.

Ru and Mo isotopic systems also offer isotopic information about genetic links between meteorite groups. Diagrams in Dauphas et al. (2004) and Fischer-Gödde et al. (2014) show the strong (negative) correlation between $\varepsilon^{100}$Ru and $\varepsilon^{92}$Mo among diverse meteorites. There are no Ru isotopic data for IIE irons in the paper by Chen et al. (2010); they summarize problems with earlier Ru data that I will not review. Burkhardt et al. (2011) measured Mo isotopes in the IIE irons Miles and Watson and found a mean $\varepsilon^{97}$Mo of $0.18 \pm 0.07$, similar to the mean of 6 OC, $0.14 \pm 0.06$. The Ru and Mo isotopic ratio data for metal 9 IIE meteorites and in Portales Valley reported by Fischer-Gödde et al. (2016) confirm that these have compositions that are the same as those in ordinary chondrites, and distinctly different from those in EL chondrites or IAB irons.

Although variations in $\varepsilon^{182}$W are mainly the result of the decay of $^{182}$Hf, in IIE irons they also offer some information about genetic clusters within the group. Fischer-Gödde et al. (2016) report cosmic-ray-exposure corrected $\varepsilon^{182}$W values for 9 IIE irons; these range from −2.1 (in Tarahumara) to −3.1 (in Barranca Blanca and Colomera). Barranca Blanca is a member of the Cu-rich set and a low value (−3.0) is also present in the other analyzed member of this set, Mont Dieu. Portales Valley metal was also analyzed; its $\varepsilon^{182}$W is −2.5, in the middle of the IIE range, consistent with the strong genetic link between IIE and H. Model ages calculated from $\varepsilon^{182}$W were briefly discussed in Section 7.

My evaluation of the $\varepsilon^{54}$Cr, $\varepsilon^{97}$Mo and $\varepsilon^{100}$Ru studies of IIE irons is that the data are consistent with the working model that IIE irons were formed by melting H or HH chondrites. Isotopic data potentially offer more quantitative links than petrological observations and elemental concentration data, but more data are still needed. A key question is whether these data (and $\Delta^{17}$O data) can be used to assess possible compositional differences between the target (probably HH) and the projectile (resolvable if it happened to differ appreciably in isotopic composition).

### 10.2. Possible limitations of $\Delta^{17}$O as an indicator of detailed genetic relationships

The range of O-isotopic compositions observed in IIE silicates by McDermott et al. (2015) is remarkably large. This (and the diversity in textures discussed above) could be used as an argument that IIE meteorites were formed on several different asteroids or (less obvious as an explanation of the O-isotope diversity) that they formed in several different impacts on the same asteroid.

Arguments against formation on several asteroids are that IIE metal occupies a rather small niche in the compositional space occupied by the full set of iron meteorites and that their Ru and Mo isotopic compositions are closely similar. Their combination of a unique bulk composition and an impact heating mechanism already makes them an unusual kind of material. It thus seems implausible that this same combination of processes occurred on two or three asteroids but still produced the relatively tight compositional clusters. I therefore conclude that (if no sample mislabeling has occurred) the O-isotope variations must be explained by materials accreted to and processes occurring on a single asteroid.

As discussed above, in an attempt to account for the scatter in O-isotopes McDermott et al. (2015) suggested that the impacted target materials consisted of unequilibrated chondrites which are known to have variable isotopic compositions (Clayton et al., 1991) and frequently also lower $\Delta^{17}$O values than their equilibrated compatriots. This explanation can work for impact melts on a single asteroid providing the melts only sample regions having sizes small enough to preserve heterogeneities (perhaps one to several millimeters). I conclude that, with this size restriction, the McDermott et al. (2015) scenario provides the best working model. Unfortunately, this conclusion also shows that $\Delta^{17}$O in small samples produced by impacts on unequilibrated chondrite targets cannot provide quantitative estimates of the bulk composition of the original target materials and thus will not always yield quantitative links to related kinds of meteorites (i.e., different groups of OC). It is thus essential to study aliquots of larger (gram-size) samples. Unanswered is the question of why the McDermott and Clayton $\Delta^{17}$O values in Colomera (four samples were analyzed at Open. Univ.) differ by more than expected from the precisions commonly achieved by the two labs.

### 10.3. Formation ages of IIE irons

There is a moderate amount of formation- and impact-melting-age data for the IIE meteorites. Interestingly, they form two clusters: one is about 4.5 Ga, close to the age of the solar system, the second is about 3.6 Ga, much later but within a relatively common age range for impact-melted (or impact-altered) meteorites (e.g., Ruzicka, 2014). Cooling rates during the temperature range where the Widmanstätten pattern formed were much higher in the younger set, implying that the insulating cover of regolith was much thinner after the later event. Interestingly, the irons with low formation/impact ages (Watson, Kodaikanal and Netschaevo) have similar contents in metal of Au, Co, and most other elements, consistent with their having originated in a single impact event into Netschaevo-like materials.

## 11. SUMMARY AND CONCLUSIONS

There are two groups of silicate-bearing non-magmatic iron meteorites, both having mainly formed by impact melting and mixing. In the larger group IAB-MG (and the low-Au IAB subgroups) the silicates have compositions that are roughly chondritic and shapes that are generally fragmental. In the smaller nonmagmatic group IIE the silicate compositions are generally less chondritic (typical compositions are plagioclase rich) and typical shapes are globular or stringer-like; glass is a common constituent. However, a few IIE meteorites (e.g., Netschaevo) contain centimeter-size chondritic fragments.

Instrumental neutron-activation (INAA) data for metal in IIE irons show narrow ranges in Ir and other refractory siderophiles; the Ir range is a factor of 2.6, a factor of ~2 smaller than in IAB-MG, and orders of magnitude smaller than in the large magmatic groups. The absence of appreciable Ir fractionation probably indicates that the melts crystallized too quickly to allow fractional crystallization. The low Ir concentration in one IIE (Miles) could reflect a minor heterogeneity in target materials. Despite the absence of fractional crystallization, the Au range is large (a factor of 2); this may reflect differential sampling of different nebular components during impact melting or, conceivably, might reflect differences in Au/Fe ratios between target and projectile.

The data reveal that the IIE irons can be split into two sets, a larger main-set and a set of 6 (or 7) Cu- (or FeS-) rich irons. The sets are also resolved on a Sb–Au diagram and largely resolved on a Ga-Au diagram. The compositions

of metal veins from the Portales Valley H chondrite plot within IIE element-Au fields with the exceptions of Co (high) and Ga (low). It is probable that the two sets of IIE irons formed together on the same asteroid. The high- and low-Cu sets may have been formed in the same impact event; the differences may partly reflect local differences in the kinetics of melt generation or in the cooling rates of the metallic melts.

H-group-chondrite- and Au-normalized IIE abundances for siderophiles show that IIE irons are ~ 30% higher than H in refractory siderophiles Re, Ir and W and are about 30% lower than H in the volatiles Ga and Sb, inconsistent with proposals that IIE irons formed from H chondrites. The IIE elemental fractionations contrast with those in bulk L chondrites which are about 15% lower than H in the three refractory elements and 40% higher than H in volatiles. These fractionations are consistent with the interpretation of Müller et al.(1971) and Wasson (1972) that OC groups represent an incompletely sampled continuous-fractionation sequence of closely related chondritic materials. it appears that the meteorites formed by melting of precursor materials similar to the chondritic blocks in Netschaevo, though unequilibrated and much more porous.

The silicate-bearing IIE irons can be divided into older and younger sets based on formation (largely $^{39}Ar$–$^{40}Ar$) ages. Similar metal compositions in the three irons with younger ages suggest formation by an impact that affected only a different part of the IIE terrain from that impacted 0.9 Ga earlier. Neither impace produced global melting thus both could have occurred on the same asteroid.

Model ages based on $\varepsilon^{182}W$ (Fischer-Gödde et al., 2016) are 4 Ma or higher, too high to be consistent with melting and phase separation powered by the decay of $^{26}Al$. This implies that the melting was the result of impacts.

Oxygen isotope data show a close relationship between IIE irons and reduced OC (the H group and an HH grouplet). McDermott et al. (2015) found a large range in $\Delta^{17}O$ with the highest value (in Colomera) close to the L-group range, ~0.3‰ higher than the Clayton et al. (1991) value. Although Open-University $\Delta^{17}O$ values in Colomera are close to the L chondrite field, its siderophile abundance ratios in metal (e.g., Ir/Au) are HH-like. The lowest $\Delta^{17}O$ values are in IIE meteorites (e.g., Netschaevo) with large, equilibrated chondritic inclusions; they appear to be well-resolved from the H-chondrite field. Thus supports the conclusion that they are representative of the materials impact melted to form IIE meteorites.

The $\varepsilon^{54}Cr$, $\varepsilon^{100}Ru$ and $\varepsilon^{92}Mo$ data for IIE irons are similar to OC values, consistent with their formation by impact melting or an H- or HH-like asteroid. Because the chemical and isotopic composition of IIE silicates indicates an HH (or H) affinity and the stable isotopes indicate an ordinary chondrite origin, it seems probable that the IIE meteorites were produced by impacts onto an HH asteroid with composition similar to Netschaevo. However, the asteroid may have been unequilibrated, with elements still in the phases that formed in the nebula, and may have had a high porosity, as expected from the first generation of planetesimals. Conversion of impact energy to heat scales roughly as the porosity of the target and projectile.

## ACKNOWLEDGEMENTS

I thank Bastian Baecker and Junko Isa for help in the neutron activation, Lucero Villanueva and John Breen for technical help and Alan Rubin, Ed Scott, Alex Ruzicka and Dimitri Papanastassiou for consultation, advice and reviews. This research was mainly supported by NASA grants NNX13AH49G and NNX14AJ84G.

## APPENDIX A. SUPPLEMENTARY DATA

Supplementary data associated with this article can be found, in the online version, at http://dx.doi.org/10.1016/j.gca.2016.09.043.

## REFERENCES

Bence A. E. and Burnett D. S. (1969) Chemistry and mineralogy of the silicates and metal of the Kodiakanal meteorite. *Geochim. Cosmochim. Acta* **33**, 387–407.

Bild R. W. and Wasson J. T. (1977) Netschaevo: a new class of chondrite meteorite. *Science* **197**, 58–62.

Blum J. and Wurm G. (2008) The growth mechanisms of macroscopic bodies in protoplanetary disks. *Annu. Rev. Astron. Astrophys.* **46**, 21–56.

Bogard D. D., Garrison D. H. and McCoy T. J. (2000) Chronology and petrology of silicates from IIE iron meteorites: evidence of a complex parent body evolution. *Geochim. Cosmochim. Acta* **64**, 2133–2154.

Brandes E. A. and Brook G. B. (1998) *Smithells Metal Reference Book*. Butterworth-Heinemann, CA.

Buchwald V. F. (1975) *Handbook of Iron Meteorites*. California Univ. Press.

Buchwald V. F. and Clarke R. S. (1987) The Verkhne Dnieprovsk iron meteorite specimens in the Vienna collection and the confusion of Verkhne Dnieprovsk with Augustinovka. *Meteoritics* **22**, 121–134.

Bunch T. E., Keil K. and Olsen E. (1970) Mineralogy and petrology of silicate inclusions in iron meteorites. *Contrib. Mineral. Petrol.* **25**, 297–340.

Burkhardt C., Kleine T., Oberli F., Pack A., Bourdon B. and Weiler R. (2011) Molybdenum isotope anomalies in meteorites: constraints on solar nebula evolution and origin of the Earth. *Earth Planet. Sci. Lett.* **312**, 390–400.

Burnett D. S. and Wasserburg G. J. (1967) Evidence for the formation of an iron meteorite at $3.8 \times 10^9$ years. *Earth Planet. Sci. Lett.* **2**, 137–147.

Casanova I., Graf T. and Marti K. (1995) Discovery of an unmelted H-chondrite inclusion in an iron meteorite. *Science* **268**, 540–542.

Chen J. H., Papanastassiou D. A. and Wasserburg G. J. (2010) Ruthenium endemic isotope effects in chondrites and differentiated meteorites. *Geochim. Cosmochim. Acta* **74**, 3851–3862.

Choi B.-G., McKeegan K. D., Krot A. N. and Wasson J. T. (1998) Extreme oxygen-isotope compositions in magnetite from unequilibrated ordinary chondrites. *Nature* **392**, 577–579.

Clarke R. S., Buchwald V. F. and Olsen E. (1990) Anomalous ataxite from Mount Howe, Antarctica. *Meteoritics* **25**, 354.

Clayton R. N. and Mayeda T. K. (1996) Oxygen isotope studies of achondrites. *Geochim. Cosmochim. Acta* **60**, 1999–2017.

Clayton R. N., Mayeda T. K., Goswami J. N. and Olsen E. J. (1991) Oxygen isotope studies of ordinary chondrites. *Geochim. Cosmochim. Acta* **55**, 2317–2337.

Clayton R. N., Mayeda T. K., Olsen E. J. and Prinz M. (1983) Oxygen isotope relationships in iron meteorites. *Earth Planet. Sci. Lett.* **65**, 229–232.

D'Orazio M., Folco L., Chaussidon M. and Rochette P. (2009) Sahara 03505 sulfide-rich iron meteorite: evidence for efficient segregation of sulfide-rich metallic melt during high-degree impact melting of an ordinary chondrite. *Meteorit. Planet. Sci.* **44**, 221–231.

Dauphas N., Davis A. M., Marty B. and Reisberg L. (2004) The cosmic molybdenum-ruthenium isotope correlation. *Earth Planet. Sci. Lett.* **226**, 465–475.

Esbensen K. H., Buchwald V. F., Malvin D. J. and Wasson J. T. (1982) Systematic compositional variations in the Cape York iron meteorite. *Geochim. Cosmochim. Acta* **46**, 1913–1920.

Fischer-Gödde M., Kleine T., Burkhardt C. and Dauphas N. (2014) Origin of nucleosynthetic isotope anomalies in bulk meteorites: evidence from coupled Ru and Mo isotopes in acid leachates of chondrite (abstract). *Lunar Planet. Sci.* **45**, 2409pdf.

Fischer-Gödde M., Kruijer T. S., Kleine T. and Wasson J. T. (2016) W, Pt, Mo and Ru isotope systematics of IIE iron meteorites (abstract). *Lunar Planet. Sci.* **47**, 2704pdf.

Göpel C., Manhes G. and Allegre C. J. (1985) Concordant 3,676 Myr U–Pb formation age for the Kodaikanal iron meteorite. *Nature* **317**, 341–344.

Ikeda Y., Ebihara M. and Prinz M. (1997) Petrology and chemistry of the Miles IIE iron. I: Description and petrology of twenty new silicate inclusions. *Antarct. Meteorite Res.* **10**, 355–372.

Ivanova G. M. and Kuznetsova I. K. (1976) The Tobychan iron meteorite (in Russian). *Meteoritika* **35**, 47–52.

Jarosewich E. (1990) Chemical analyses of meteorites: a compilation of stony and iron meteorite analyses. *Meteoritics* **25**, 323–337.

Kallemeyn G. W., Rubin A. E., Wang D. and Wasson J. T. (1989) Ordinary chondrites: Bulk compositions, classification, lithophile-element fractionations, and composition-petrographic type relationships. *Geochim. Cosmochim. Acta* **53**, 2747–2767.

Keil K., Stöffler D., Love S. G. and Scott E. R. D. (1997) Constraints on the role of impact heating and melting in asteroids. *Meteorit. Planet. Sci.* **32**, 349–363.

Kita N. T. and Ushikubo T. (2012) Evolution of protoplanetary disk inferred from $^{26}$Al chronology of individual chondrules. *Meteorit. Planet. Sci.* **47**, 1108–1119.

Kring D. A., Hill D. H., Gleason J. D., Britt D. T., Consolmagno G. J., Farmer M., Wilson S. and Haag R. (1999) Portales Velley: a meteoritic sample of the brecciated and metal-veined floor of an impact crater on an H-chondrite asteroid. *Meteorit. Planet. Sci.* **34**, 663–669.

Kunihiro T., Rubin A. E., McKeegan K. and Wasson J. T. (2004) Initial $^{26}$Al/$^{27}$Al in carbonaceous-chondrite chondrules: too little $^{26}$Al to melt asteroids. *Geochim. Cosmochim. Acta* **68**, 2947–2957.

Malvin D. J., Wang D. and Wasson J. T. (1984) Chemical classification of iron meteorities–X. Multielement studies of 43 irons, resolution of group IIIE from IIIAB, and evaluation of Cu as a taxonomic parameter. *Geochim. Cosmochim. Acta* **48**, 785–804.

McDermott K. H., Greenwood R. C., Scott E. R. D., Franchi I. A. and Anand M. (2015) Oxygen isotope and petrological study of silicate inclusions in IIE iron meteorites and their relationship with H chondrites. *Geochim. Cosmochim. Acta* **173**, 97–113.

Müller O., Baedecker P. A. and Wasson J. T. (1971) Relationship between siderophilic-element content and oxidation state of ordinary chondrites. *Geochim. Cosmochim. Acta* **35**, 1121–1137.

Olsen E. and Jarosewich E. (1971) Chondrules: first occurrence in an iron meteorite. *Science* **174**, 583–585.

Olsen E. J., Davis A., Clarke R. S., Schultz L., Weber H., Clayton R. N., Mayeda T., Jarosewich E., Sylvester P., Grossman L., Wang M.-S., Lipschutz M. E., Steele I. M. and Schwade J. (1994) Watson: a new link in the IIE iron chain. *Meteoritics* **29**, 200–213.

Osadchii E. G., Baryshnikova G. V. and Novikov G. V. (1981) The Elga meteorite: silicate inclusions and shock metamorphism. *Proc. Lunar Planet. Sci.* **12B**, 1049–1068.

Ray D., Ghosh S. and Murty S. V. S. (2014) Shock-thermal history of Kavarpura (IVA) iron: Evidences from microtextures and nickel profiling (abstract). *Meteorit. Soc. Ann. Mtg.* **77**, 5157.pdf.

Rubin A. E. (1995) Fractionation of refractory siderophile elements in metal from the Rose City meteorite. *Meteoritics* **30**, 412–417.

Rubin A. E., Ulff-Møller F., Wasson J. T. and Carlson W. D. (2001) The Portales Valley meteorite breccia: evidence for impact-induced melting and metamorphism of an ordinary chondrite. *Geochim. Cosmochim. Acta* **65**, 323–342.

Ruzicka A. (2014) Silicate-bearing iron meteorites and their implications for the evolution of asteroidal parent bodies. *Chem. Erde* **74**, 3–48.

Ruzicka A., Fowler G. W., Snyder G. A., Prinz M., Papike J. J. and Taylor L. A. (1999) Petrogenesis of silicate inclusions in the Weekeroo Station IIE iron meteorite: Differentiation, remelting, and dynamic mixing. *Geochim. Cosmochim. Acta* **63**, 2123–2143.

Ruzicka A. and Hutson M. (2010) Comparative petrology of silicates in the Udei Station (IAB) and Miles (IIE) iron meteorites: implications for the origin of silicate-bearing irons. *Geochim. Cosmochim. Acta* **74**, 394–433.

Ruzicka A., Killgore M., Mittlefehldt D. W. and Fries M. D. (2005) Portales Valley: petrology of a metallic-melt meteorite breccia. *Meteorit. Planet. Sci.* **40**, 261–295.

Schramm D. N., Tera F. and Wasserburg G. J. (1970) The isotopic abundance of $^{26}$Mg and limits on $^{26}$Al in the early solar system. *Earth Planet. Sci. Lett.* **10**, 44–59.

Scott E. D. and Wasson J. T. (1975) Classification and properties of iron meteorites. *Rev. Geophys. Space Phys.* **13**, 527–546.

Scott E. R. D. and Wasson J. T. (1976) Chemical classification of iron meteorites–VIII. Groups IC, IIE, IIIF and 97 other irons. *Geochim. Cosmochim. Acta* **40**, 103–115.

Takeda H., Bogard D. D., Otsuki M. and Ishii T. (2003) Mineralogy and Ar-Ar age of the Tarahumara IIE iron, with reference to the origin of alkali-rich materials (abstract). Internat. Symp. Evolution of Solar System Materials: A New Perspective from Antarctic Meteorites. *Nat. Inst. Polar Res.*, 134–135.

Tang H. and Dauphas N. (2015) Low $^{60}$Fe abundance in Semarkona and Sahara 99555. *Astrophys. J.* **802**(22), 1.

Telus M., Huss G. R., Ogliore R. C., Nagashima K., Howard D. L., Newville M. G. and Tomkins A. G. (2016) Mobility of iron and nickel at low temperatures: implications for $^{60}$Fe–$^{60}$Ni systematics of chondrules from unequilibrated ordinary chondrites. *Geochim. Cosmochim. Acta* **178**, 87–105.

Terasaki H., Suzuki A., Ohtani E., Nishida K., Sakamaki T. and Funakoshi K. (2006) Effect of pressure on the viscosity of Fe–S and Fe–C liquids up to 16 GPa. *Geophys. Res. Lett.* **33**, L22307.

Trinquier A., Birck J. and Allegre C. J. (2007) Widespread $^{54}$Cr heterogeneity in the inner solar system. *Astrophys. J.* **655**, 1179–1185.

Van Roosbroek N., Debaille V., Pittarello L., Goderis S., Humayun M., Hecht L., Jourdan F., Spicuzza M. J., Vanhaecke F. and Claeys P. (2015) The formation of IIE iron meteorites investigated by the chondrule-bearing Mont Dieu meteorite. *Meteorit. Planet. Sci.* **50**, 1173–1196.

Van Roosbroek N., Pittarello L., Greshake A., Debaille V. and Claeys P. (2016) First finding of impact melt in the IIE Netschaëvo meteorite. *Meteorit. Planet. Sci.* **51**, 1–18.

Wasserburg G. J., Sanz H. G. and Bence A. E. (1968) Potassium feldspar phenocrysts in the surface of Colomera, an iron meteorite. *Science* **161**, 684–687.

Wasson J. T. (1970) The chemical classification of iron meteorites–IV. Irons with Ge concentrations greater than 190 ppm and other meteorites associated with group I. *Icarus* **12**, 407–423.

Wasson J. T. (1972) Formation of ordinary chondrites. *Rev. Geophys. Space Phys.* **10**, 711–759.

Wasson J. T. (1999) Trapped melt in IIIAB irons; solid/liquid elemental partitioning during the fractionation of the IIIAB magma. *Geochim. Cosmochim. Acta* **63**, 2875–2889.

Wasson J. T., Huber H. and Malvin D. J. (2007) Formation of IIAB iron meteorites. *Geochim. Cosmochim. Acta* **71**, 760–781.

Wasson J. T. and Kallemeyn G. W. (1988) Compositions of chondrites. *Philos. Trans. R. Soc. London* **A325**, 535–544.

Wasson J. T. and Kallemeyn G. W. (2002) The IAB iron-meteorite complex: a group, five subgroups, numerous grouplets, closely related, mainly formed by crystal segregation in rapidly cooling melts. *Geochim. Cosmochim. Acta* **66**, 2445–2473.

Wasson J. T., Matsunami Y. and Rubin A. E. (2006) Silica and pyroxene in IVA irons; possible formation of the IVA irons by impact melting and reduction of L-LL chondrite parental materials followed by crystallization and cooling. *Geochim. Cosmochim. Acta* **70**, 3149–3172.

Wasson J. T., Ouyang X., Wang J. and Jerde E. (1989) Chemical classification of iron meteorites: XI. Multi-element studies of 38 new irons and the high abundance of ungrouped irons from Antarctica. *Geochim. Cosmochim. Acta* **53**, 735–744.

Wasson J. T. and Richardson J. W. (2001) Fractionation trends among IVA iron meteorites: contrasts with IIIAB trends. *Geochim. Cosmochim. Acta* **65**, 951–970.

Wasson J. T. and Wang J. (1986) A nonmagmatic origin of group IIE iron meteorites. *Geochim. Cosmochim. Acta* **50**, 725–732.

Winchell N. H. (1896) The Arlington iron–Minnesota No. 2. *Amer. Geol.* **18**, 267–271.

Yang J. and Goldstein J. I. (2006) Metallographic cooling rates of the IIIAB iron meteorites. *Geochim. Cosmochim. Acta* **70**, 3197–3215.

*Associate editor:* Dimitri Papanastassiou